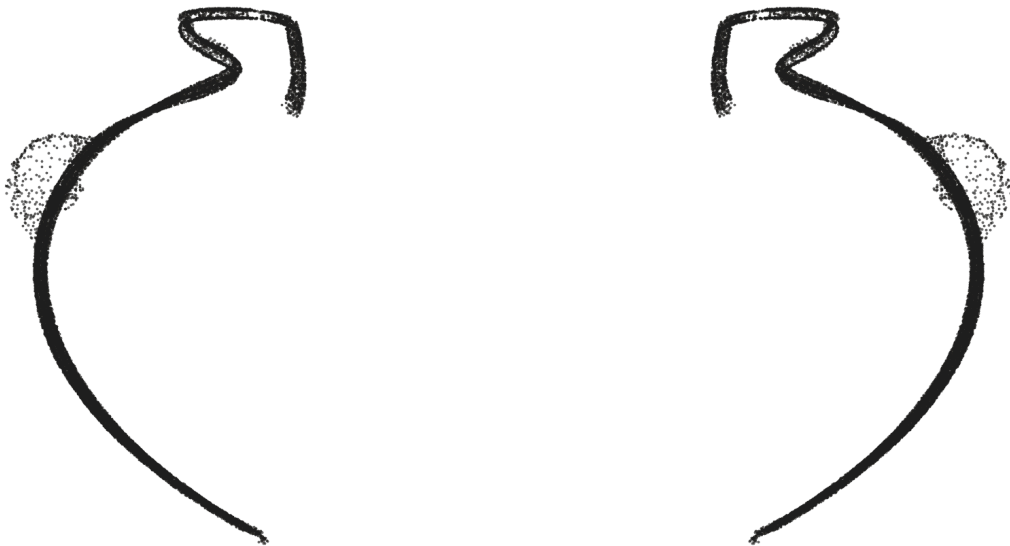


MV018 - Squat Ovoid Jar

An Exploration of Precision



Author: Stine Gerdes, arcsci.org
License: Creative Commons BY-NC-SA 4.0
Date: 2025-03-18
Version: 01.00



Petrie Museum, CC BY-NC-SA

Contents

Artifact Information	2
Alignment In The Cartesian Coordinate System	3
Precision	5
Circularity	5
Concentricity	21
Coaxiality	29
Surface Variability	32
Precision Score Of The Artifact	39
Analysis Roadmap	41
Appendix A - Comparison Of Circularity Measurements (Z-plane vs. surface-perpendicular)	42
Appendix B - Comparison Of Concentricity Measurements (Z-plane vs. surface-perpendicular)	49

Artifact Information

Artifact Data

Collection	Petrie Museum of Egyptian Archaeology
Provenance ¹	Petrie Museum of Egyptian Archaeology (London), recovered by Flinders Petrie
Provenience ²	Naqada Cemetery T Tomb 20 (Naqada III) - Petrie Excavation
Attribution	Naqada III

Museum information

Ref.	LDUCE-UC4649
Description	Vase of diorite, squat, type 15, rim and one handle broken. From Naqada Cemetery T Tomb 20
URL	https://collections.ucl.ac.uk/Details/collect/7162

Maijers vessel classification³

Short classification	Squat Ovoid Jar
Long classification	The vessel is created in a closed form classified as a squat jar with a ovoid shape, a rounded rim.

Physical properties

Precision score ⁴	12
Height (approximate)	41 mm 1.61 in
Width (approximate)	72 mm 2.83 in
Material	Diorite
Mohs Hardness ⁵	5.5 - 7 (Diorite)
Weight	

Scan information

Source	Scanned by Artifact Foundation
Source file name	UC4649_base_0.09.stl
Scan method	Laser
Scanner	FreeScan Combo+
Rated scan accuracy	20 µm 0.82 thou
Scan date	10/7/2024
Scanned by	Adam Young, Karoly Poka

Mesh decimation	None, raw scan file used in the analysis
Number of vertices	2 226 757
Mesh density ⁶	36 µm 1.40 thou
Max vertex distance	128 µm 5.055 thou
Min vertex distance	0 µm 0.000 thou
Vertices per cm ²	20 843 (approximated)
Vertices per in ²	134 470 (approximated)

¹The verifiable chain of custody of an artifact

²The location or site where an artifact was recovered

³Vessel artifact classification developed by W. Arnold Maijer and described in his publication *Masters of Stone*, ISBN 978-90-829212-0-5

⁴The precision score metric is described in *Precision Score Of The Artifact*, p. 40

⁵The Mohs scale is an ordinal scale, from 1 to 10, describing the materials resistance to abrasion (the ability of harder material to scratch softer material)

⁶Median distance between vertices

Alignment In The Cartesian Coordinate System

For precise and valid measurements of the vessel's geometry to be possible, the points of the scanned dataset must first and foremost be placed optimally in a Cartesian coordinate system. Several alignment methods and algorithms have been tested on a number of different vessels to determine the best way to achieve optimal alignment.

Any misalignment of the artifact will increase the error of the precision measurements, due to the distortion/wobble effect caused by the misaligned object. To visualize this distortion, we can consider a representation of the three-dimensional point cloud data, folded to a two-dimensional plane. This folded representation is obtained by rotating all scanned points around an assumed center axis to $y = 0, x > 0$, thus resulting in a two-dimensional profile representation of all scanned vertices in the object.

Figure 1 illustrates this effect on a ideal ellipsoid. In the first image, the ellipsoid is perfectly aligned, resulting in a narrow and precise two-dimensional folded profile. As misalignments are introduced, the two-dimensional profile increases in width, visually showing the distortion, causing the error in the precision measurements to increase. While easy to understand visually, this distortion can also be objectively quantified, and as such used to compare the fitness of different assumed center axes against each other, and further to create an automated and solid process for optimal Cartesian alignment of the scan data.

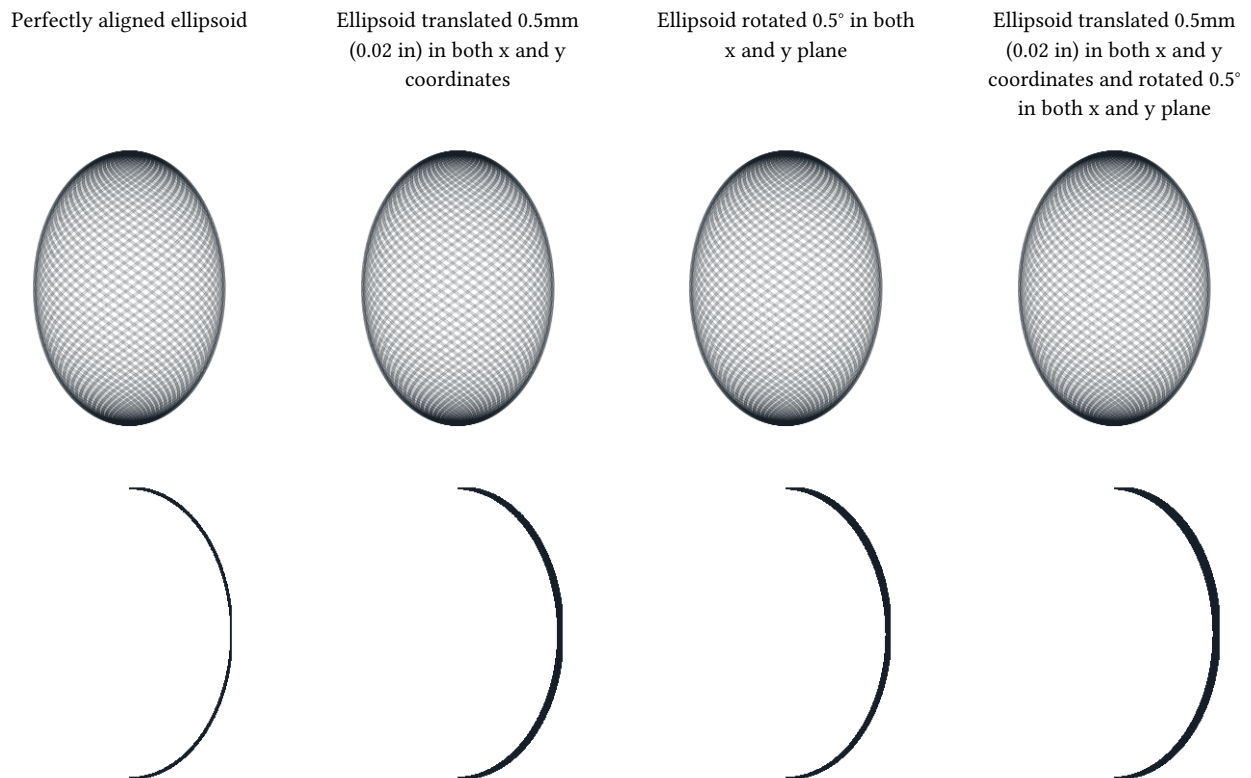


Figure 1: Distortion caused by a misalignment of the artifact

In contemporary metrology analysis of modern production objects, it is common to align the object in a Cartesian coordinate system by fitting a flat surface of the object to a reference plane in the coordinate system, cylindrical features to an ideal cylinder etc., or by using specific markers placed on the object in the design process. This methodology, however, is inadequate for the ancient objects in question. Most scanned artifacts, do not have a valid flat surface which could be aligned to a plane in the Cartesian coordinate system; most surfaces seem to be curved. Some artifacts do have a flat base, however this is often a worn area of the artifact and practical tests have shown that alignment to such surfaces will not produce optimal alignment of the scan data.

As conventional methods of alignment do not always yield good results with these types of artifacts, a more adequate method of alignment has been developed to enable precise measurements and statistical analysis of the scan data.

To find the optimal position of the vessel in the coordinate system, a range of rotation and translation tests are carried out to find the best fit of the central axis.

Based on the assumption that the analyzed object was created using a rotational process, and thus have symmetry around a central axis, the alignment of the artifact is carried out in a two-step process. An overview of this process is given below.

The artifact is placed in a Cartesian coordinate system, in an initially unaligned state. The first step in the alignment process estimates the central rotational axis of the vessel, by analyzing the coaxiality of thin cross-section slices of the vessel. The slices will be as thin as possible based on the mesh density of the scan, while still ensuring enough data points in each slice to be statistically valid.

For each slice, circular regression⁷ (estimate of best fit circle) is used to estimate the center point of this slice. Combined over the total Z-axis range of the vessel, these center points provide us with an indicator of the incline and position of the vessel's central axis.

The next step will optimize the center axis alignment by progressively minimizing the deviation (perpendicular to the surface curvature) of the two-dimensional profile, see Figure 1. By ascertaining and comparing the resulting fit of many thousands of different potential rotations, the best fit alignment of the scan data can be estimated, and an optimal center axis (in relation to the data points) can be reconstructed. The actual three-dimensional point-cloud is then aligned to this axis, by rotating and translating the scanned data points to match the Z-axis of the Cartesian coordinate system.

⁷Circle regression algorithm used: Kenichi Kanatani, Prasanna Rangarajan, "Hyper least squares fitting of circles and ellipses" Computational Statistics & Data Analysis, Vol. 55, pages 2197-2208, (2011)

Precision

To explore the manufacturing precision of the artifact in depth, the following analysis have been carried out:

- Circularity around the axis of symmetry is examined in detail at selected cross-sections.
- Overall circularity around the axis of symmetry is measured for the full height of the vessel (areas of the vessel with extensive damage are not taken into account for this metric).
- Concentricity of the vessel between selected cross-sections are examined in detail to determine if the existence of an axis of rotation in the manufacture of the object can be established.
- The coaxiality of the vessel is analyzed to explore the precision of the central axis of the object.
- The surface variability is analyzed and visualized on through a heatmap.

Circularity

Circularity is the measurement of how round the surface of an object is, optionally in reference to a datum axis. The *circularity tolerance* is the radial distance of two circles, each with their centers in the datum axis, and each of them conforming, respectively, to the minimum and maximum deviations of the data-set to a true circle, see Figure 2.

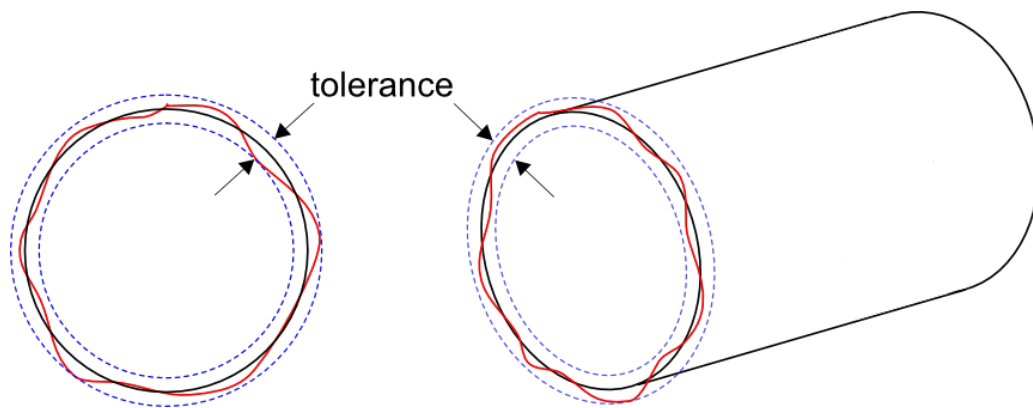


Figure 2: Circularity tolerance.

Circularity is examined at different cross-sections of the vessel, using the established Z-axis as the datum axis (axis of symmetry). The distance between the scanned points in the local datum plane is measured to determine the range between the two concentric circles encompassing the measured points, see Figure 3.

Referencing all of the individual circularity measurements to the global (reconstructed) axis of symmetry of the object, allows us to ascertain not only circularity of local features of the object, but how well circularity was *maintained* over the entire manufacturing process. This is an important distinction, which may be able to provide valuable insights into requirements of the construction methods. For reference, and seeing that the variance in local circularity also holds interest, measurements of circularity of the vessel without reference to the axis of symmetry can additionally be found in the Concentricity, p. 22.

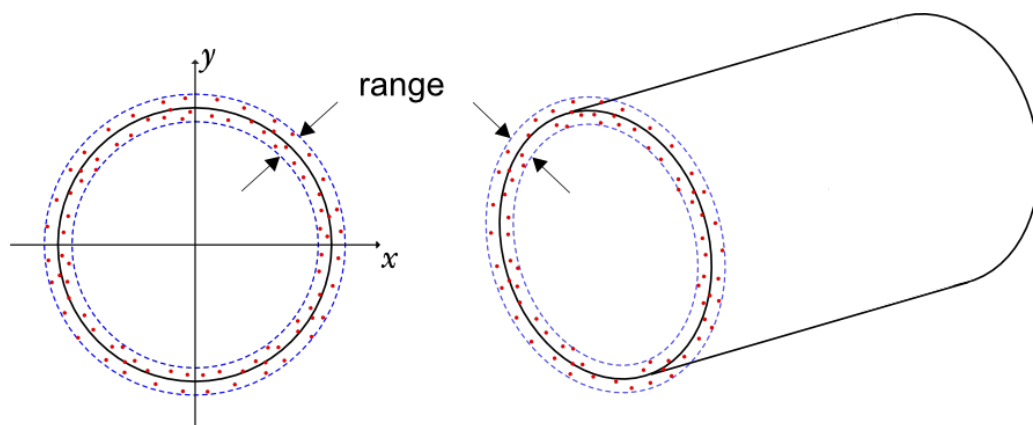


Figure 3: Circularity measurements.

If the circularity is determined from slices of the vessel exclusively in the *Z-plane* (actually measuring the cylindricality of a very thin slices of the vessel, in an attempt to approximate circularity), this would - in some areas - introduce significant distortion (increasing measurement errors) in the samples, due to the curvature of the vessel's surface.

Each sample slice of the vessel is therefore obtained perpendicular to the surface curvature, see Figure 5 to Figure 10. The measurements are taken conservatively without filtration of potential outliers.

To explore the potential distortion caused by obtaining samples in the Z-plane only, please refer to Appendix A, where measurements in the Z-plane and measurements perpendicular to surface curvature are compared side by side.

Detailed circularity measurements of selected points

Circularity measurements across a range of selected slices of the vessel (see Table 1) have been analyzed in-depth, and detailed plots of each measurement is provided. Furthermore, full circularity measurements are shown for each available scanned surface including a detailed plot to visualize the circularity of all areas of the vessel.

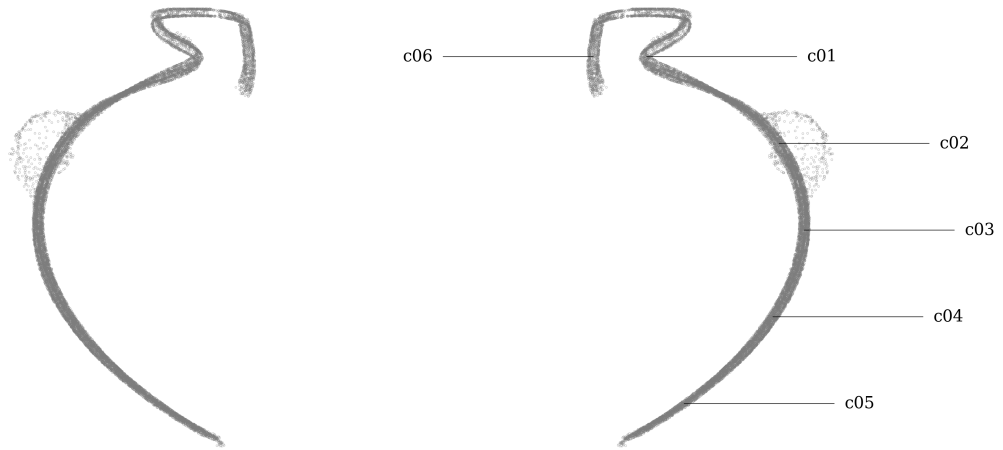


Figure 4: Circularity measurement sample location on MV018.

Metric

Tag	Area	Measured deviation ⁸	Residuals				Sample size	Slice		
			Range	RMSD ⁹	MAD ¹⁰	SD		Height	Z coord.	Radius ¹¹
		mm	mm	mm	mm	mm	mm	mm	mm	
c01	exterior	Ø42.190±0.667	1.113	0.329	0.268	0.329	1315	0.050	36.506	21.095
c02	exterior	Ø66.957±0.623	1.089	0.291	0.191	0.291	1286	0.050	28.418	33.478
c03	exterior	Ø71.663±0.506	1.000	0.282	0.241	0.282	2073	0.050	20.329	35.831
c04	exterior	Ø65.802±0.484	0.924	0.272	0.248	0.272	1656	0.050	12.241	32.901
c05	exterior	Ø49.198±0.432	0.706	0.148	0.099	0.148	850	0.050	4.152	24.599
c06	interior	Ø32.203±0.545	1.070	0.349	0.354	0.349	942	0.050	36.506	16.102

Imperial

Tag	Area	Measured deviation ⁸	Residuals				Sample size	Slice		
			Range	RMSD ⁹	MAD ¹⁰	SD		Height	Z coord.	Radius ¹¹
		in	in	in	in	in	in	in	in	
c01	exterior	Ø1.6610±0.0262	0.0438	0.0129	0.0106	0.0129	1315	0.0020	1.4373	0.8305
c02	exterior	Ø2.6361±0.0245	0.0429	0.0114	0.0075	0.0114	1286	0.0020	1.1188	1.3180
c03	exterior	Ø2.8214±0.0199	0.0394	0.0111	0.0095	0.0111	2073	0.0020	0.8004	1.4107
c04	exterior	Ø2.5906±0.0191	0.0364	0.0107	0.0098	0.0107	1656	0.0020	0.4819	1.2953
c05	exterior	Ø1.9369±0.0170	0.0278	0.0058	0.0039	0.0058	850	0.0020	0.1635	0.9685
c06	interior	Ø1.2678±0.0215	0.0421	0.0137	0.0139	0.0137	942	0.0020	1.4373	0.6339

Table 1: Detailed circularity measurements at selected samples of MV018.

Figure 5 to Figure 10 shows a detailed plots of each circularity measurement.

⁸Sample diameter Ø± maximum measured deviation from measured radius

⁹Root mean square deviation (RMSD) also called Root mean square error (RMSE)

¹⁰Median absolute deviation

¹¹Median sample radius from z-axis

Graphical overview of circularity measurement c01

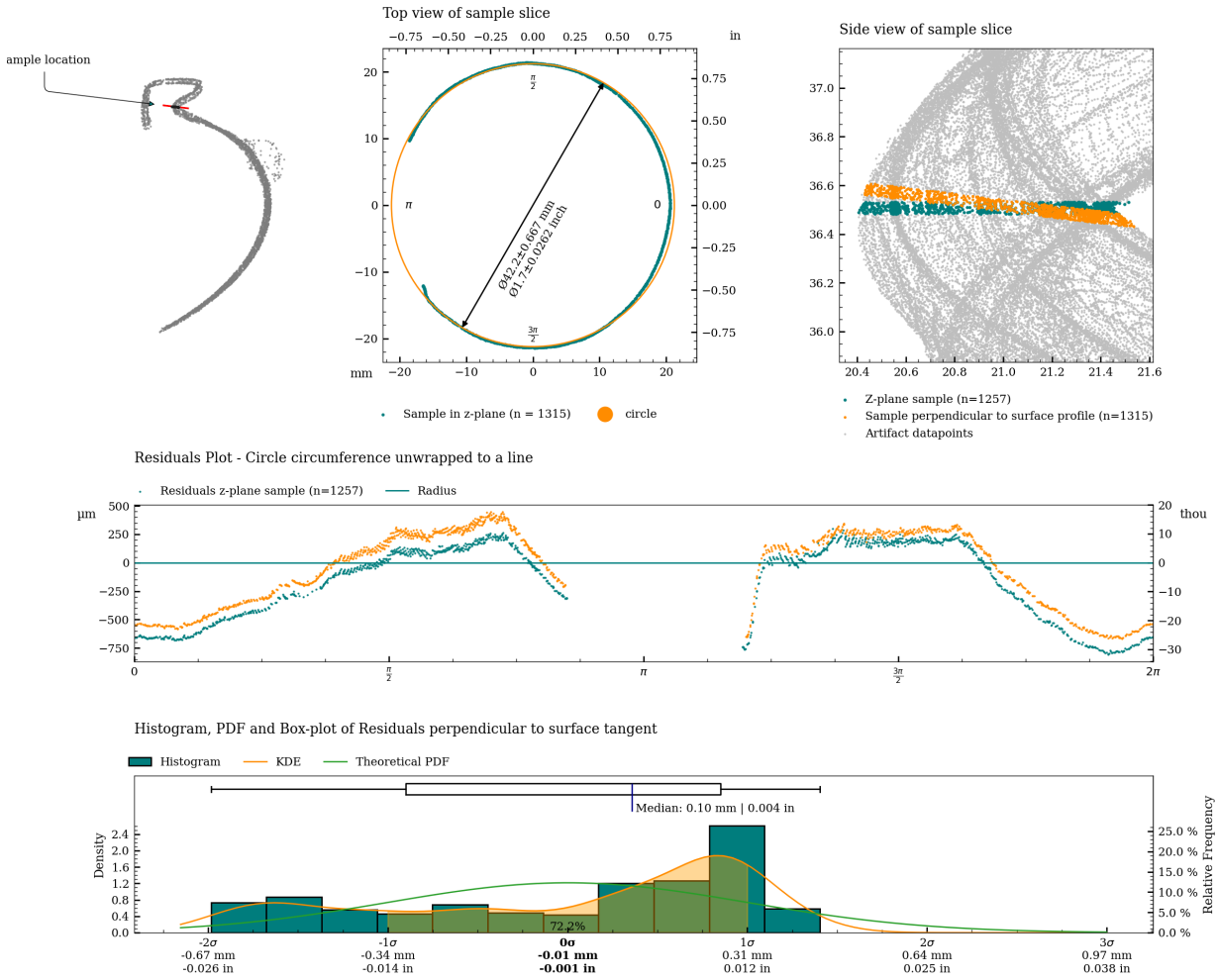


Figure 5: Charts with statistics for the measurement of c01.

Graphical overview of circularity measurement c02

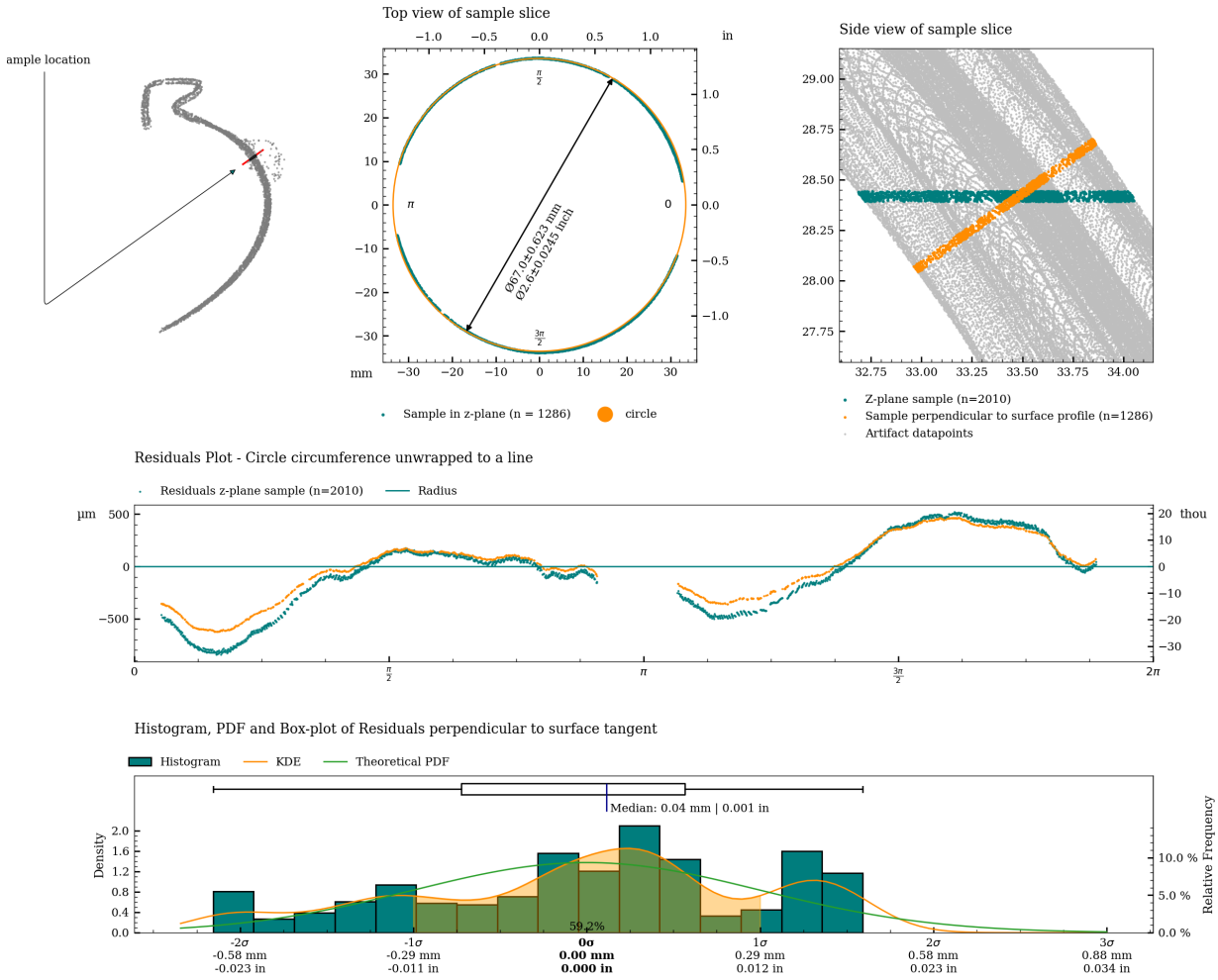


Figure 6: Charts with statistics for the measurement of c02.

Graphical overview of circularity measurement c03

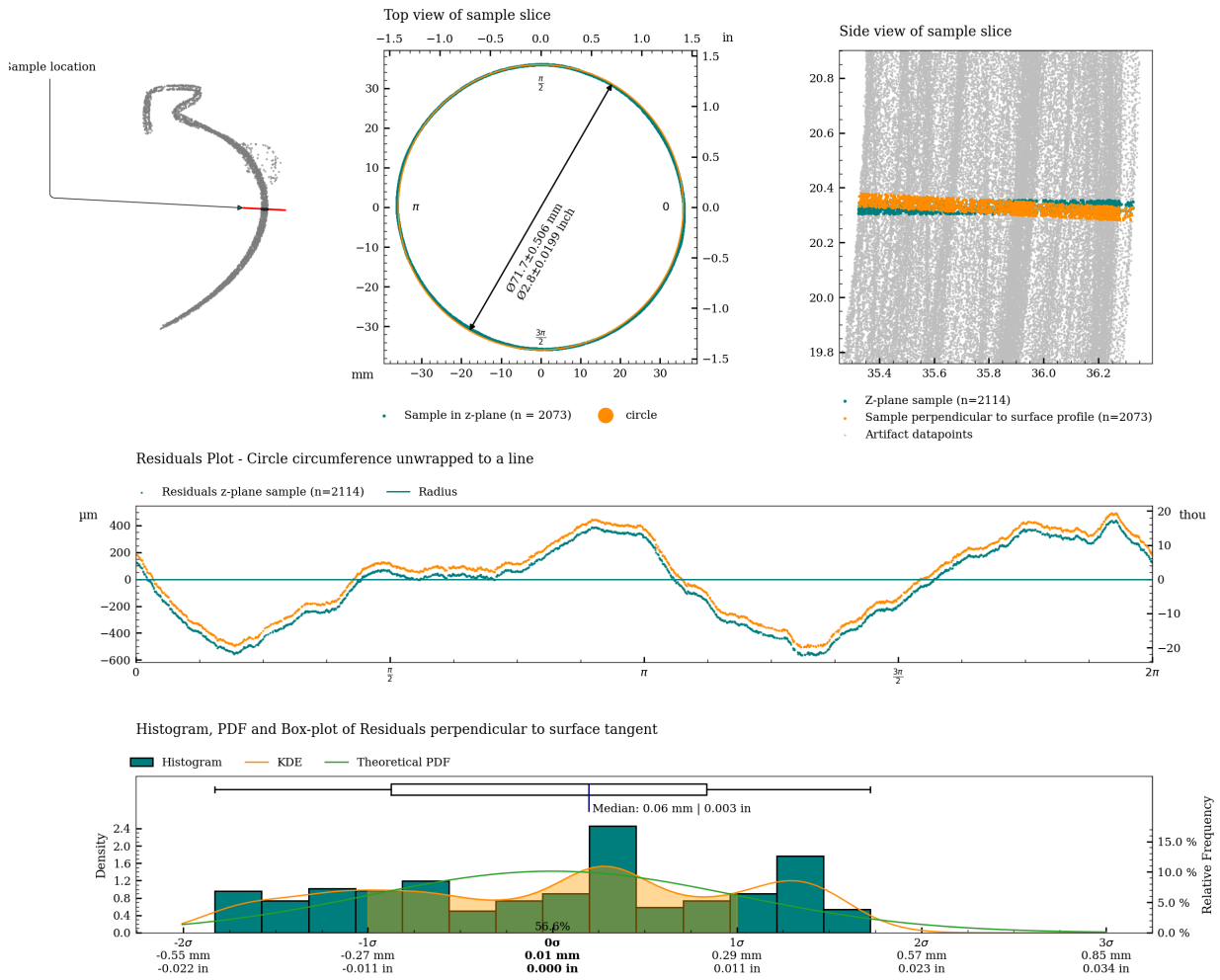


Figure 7: Charts with statistics for the measurement of c03.

Graphical overview of circularity measurement c04

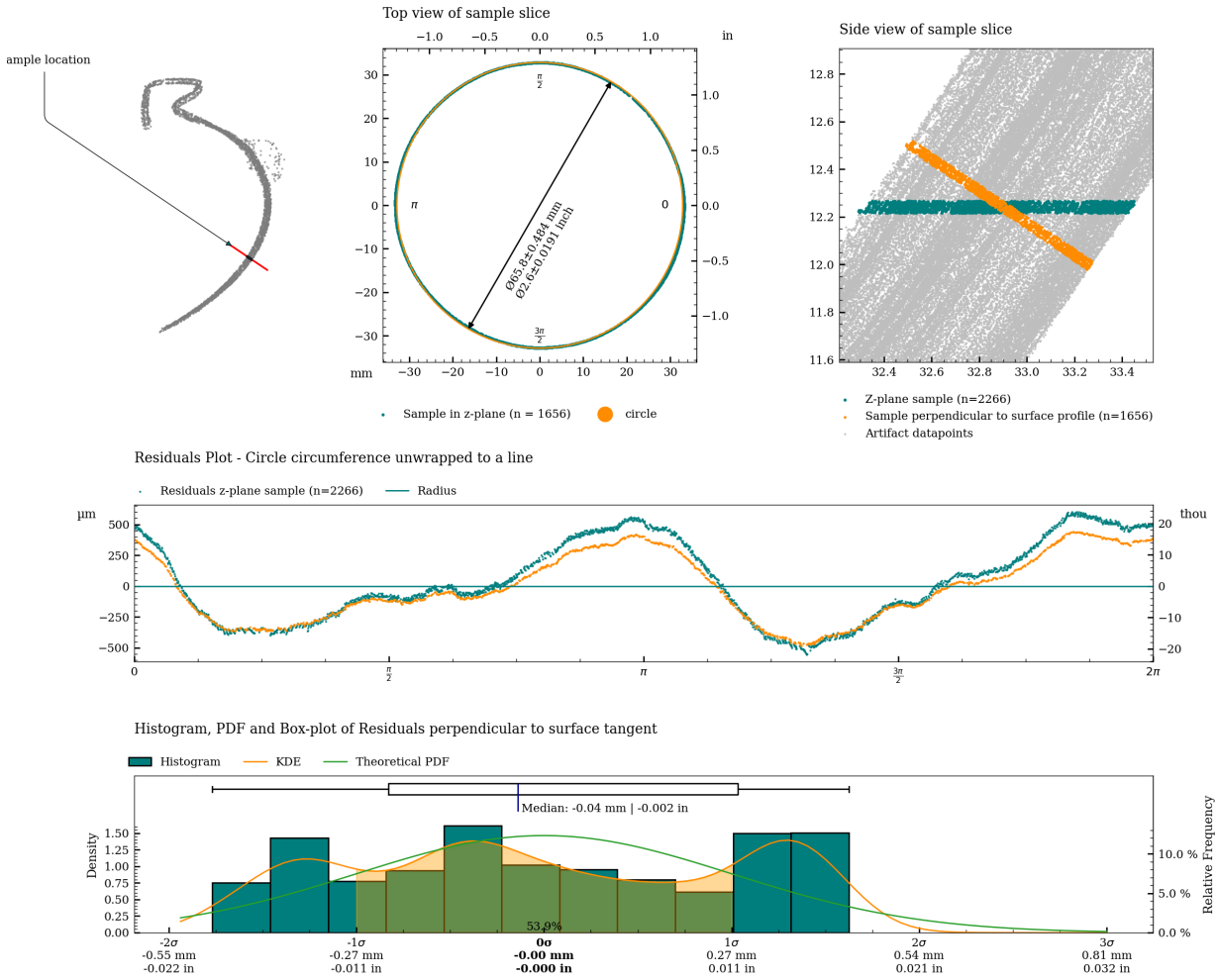


Figure 8: Charts with statistics for the measurement of c04.

Graphical overview of circularity measurement c05

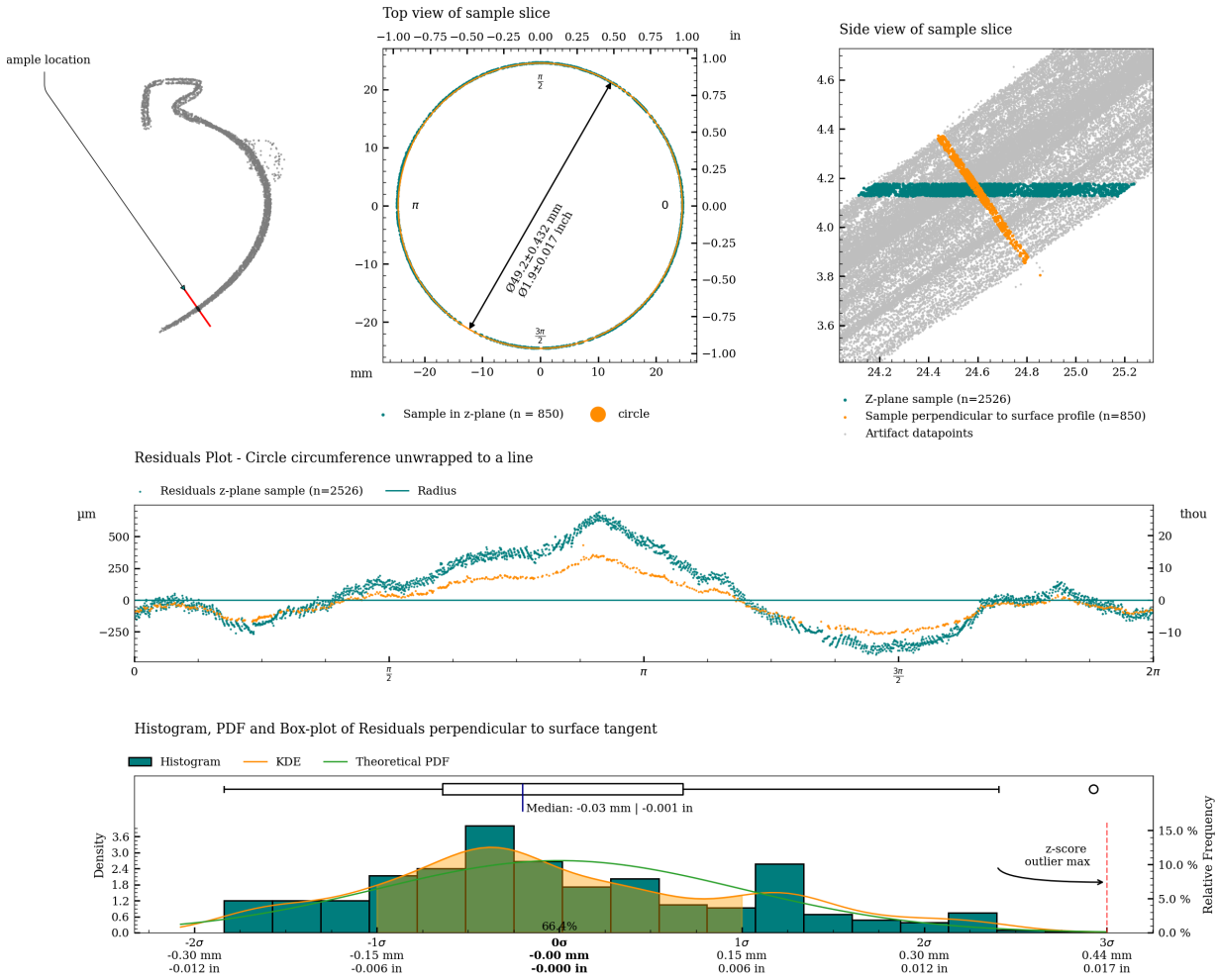


Figure 9: Charts with statistics for the measurement of c05.

Graphical overview of circularity measurement c06

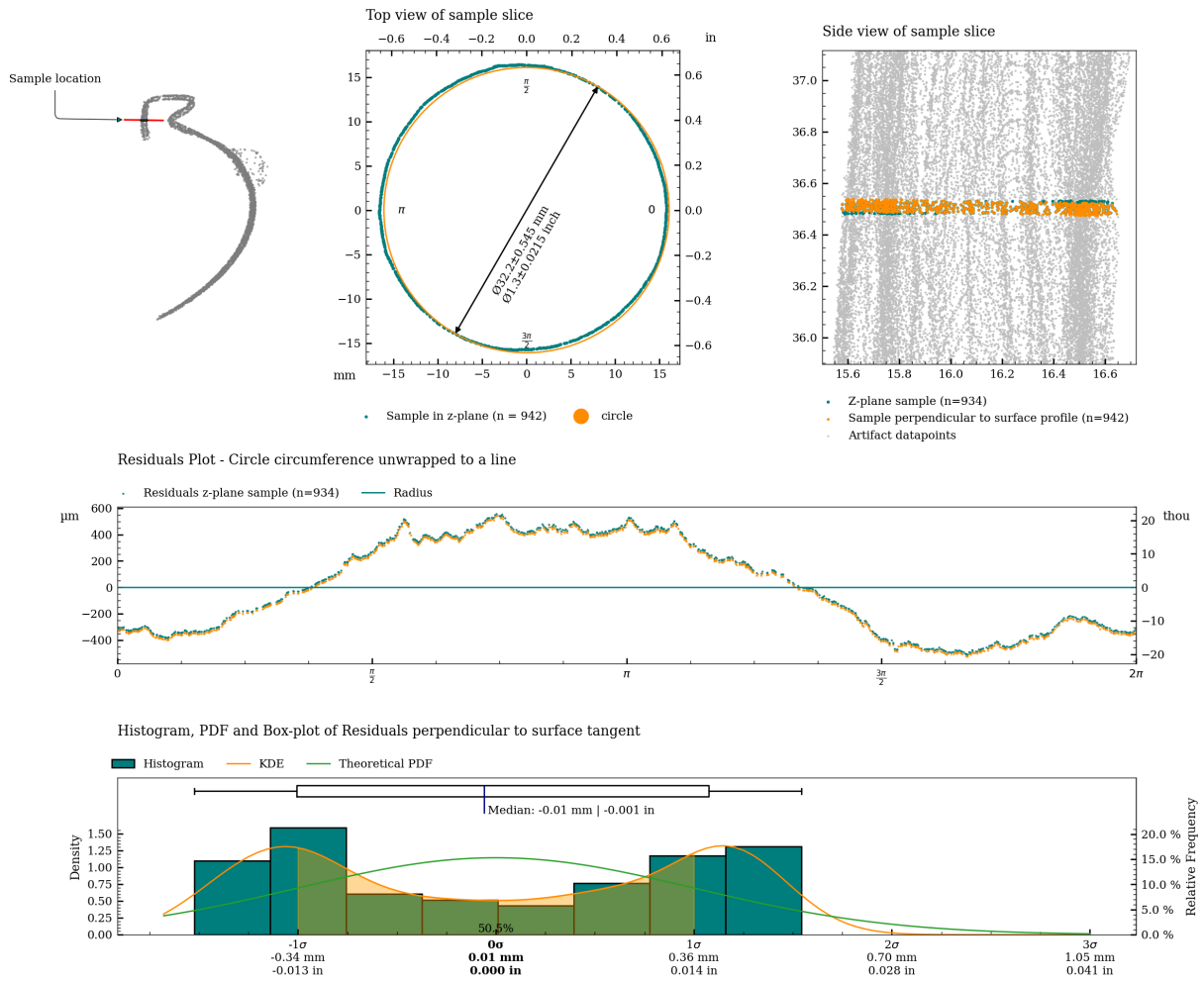


Figure 10: Charts with statistics for the measurement of c06.

Table 2 shows statistical measures of the circularity of the vessel, measured along the full height (damaged parts may reduce the measurement area).

Metric

Area	Range			Standard Deviation			Median Absolute Deviation			Slices	Slice height
	Median	Min.	Max.	Median	Min.	Max.	Median	Min.	Max.		
	mm	mm	mm	mm	mm	mm	mm	mm	mm		mm
Exterior	1.007	0.476	1.526	0.274	0.122	0.391	0.024	0.082	0.257	721	0.050
Interior	1.074	0.920	1.701	0.346	0.299	0.449	0.021	0.206	0.387	120	0.050

Imperial

Area	Range			Standard Deviation			Median Absolute Deviation			Slices	Slice height
	Median	Min.	Max.	Median	Min.	Max.	Median	Min.	Max.		
	in	in	in	in	in	in	in	in	in		in
Exterior	1.007	0.476	1.526	0.274	0.122	0.391	0.024	0.082	0.257	721	0.050
Interior	1.074	0.920	1.701	0.346	0.299	0.449	0.021	0.206	0.387	120	0.050

Table 2: Perpendicular Circularity analysis of MV018.

Circularity analysis of exterior surface

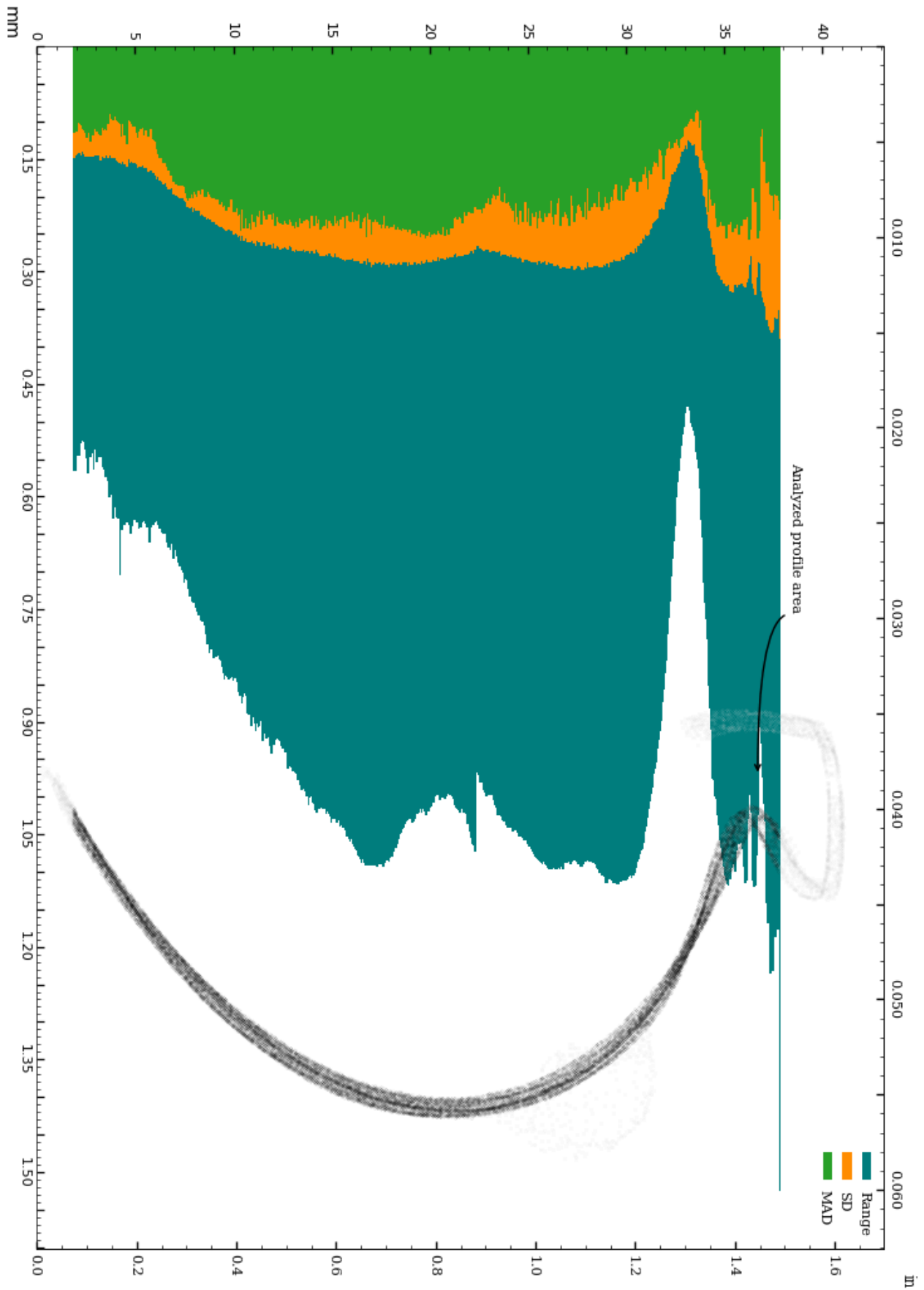


Figure 11: Circularity of exterior surface.

Circularity analysis of exterior surface, Standard Deviation and Median Absolute Deviation

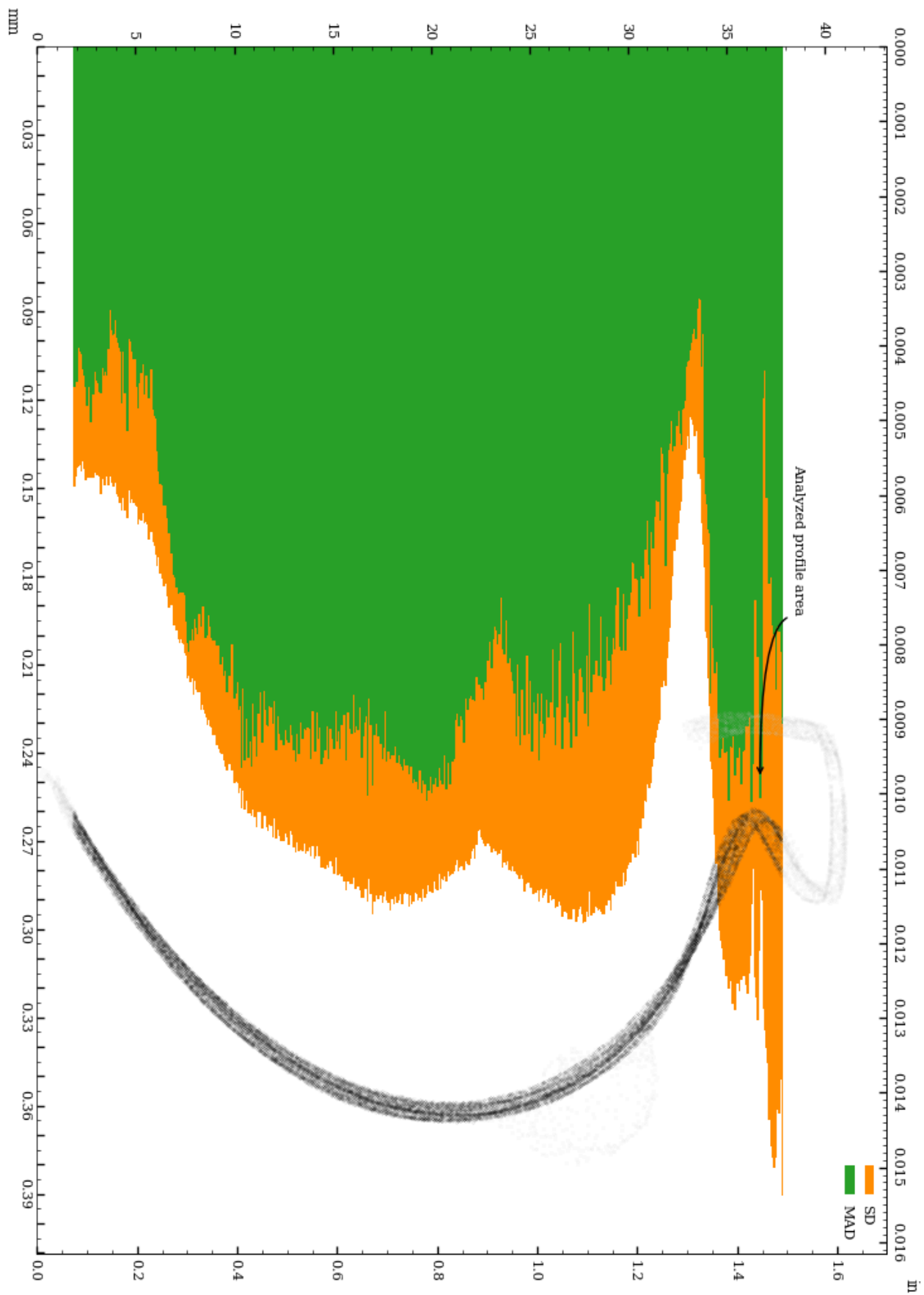


Figure 12: Vessel circularity of exterior surface, standard deviation and median absolute deviation.

The distributions of the circularity measurements across 721 slices of the exterior surface are shown below.

Range measurement distribution across 721 slices of exterior surface

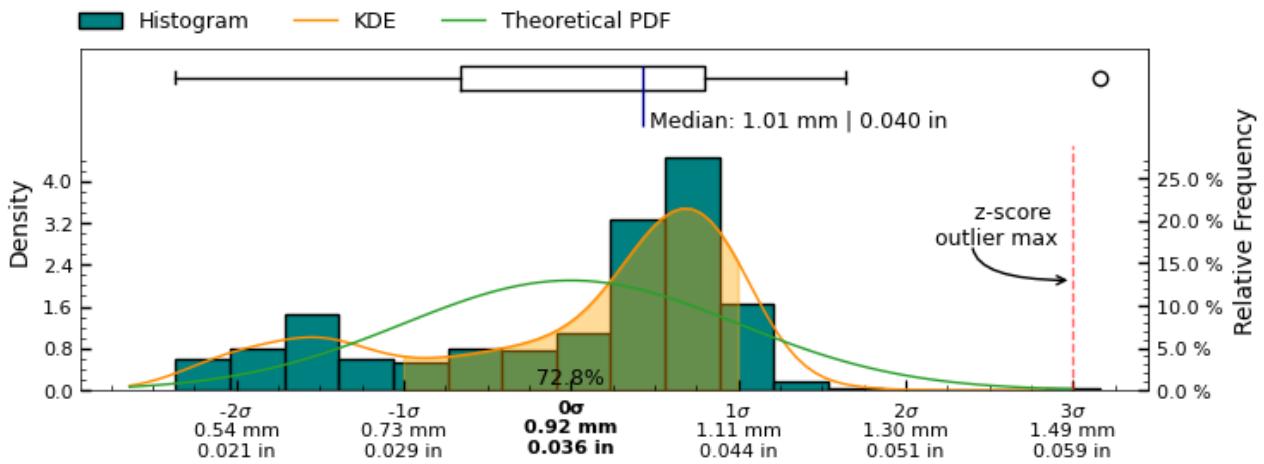


Figure 13: Range measurement distribution across measured slices of exterior surface

Standard deviation measurement distribution across 721 slices of exterior surface

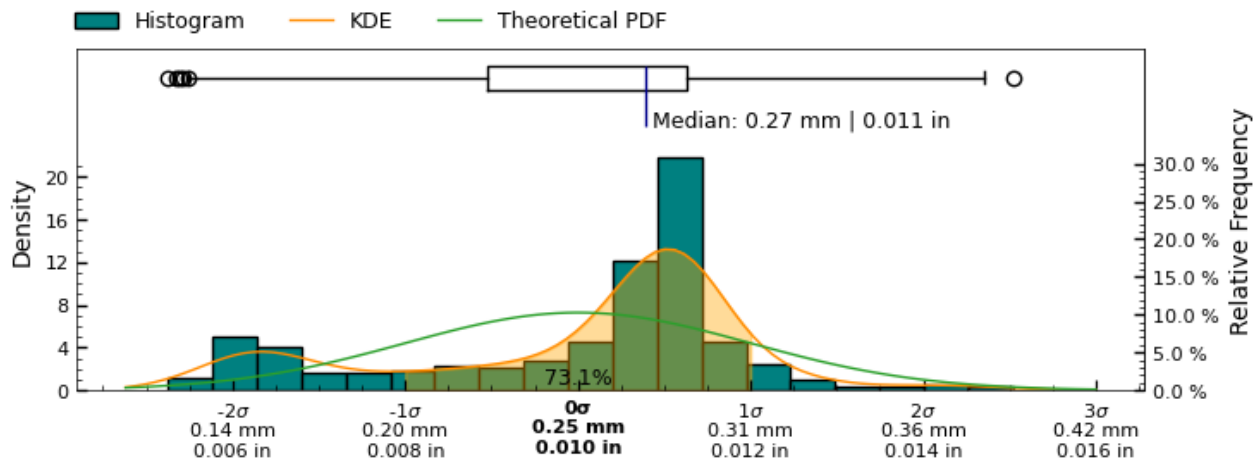


Figure 14: Standard deviation measurement distribution across measured slices of " + exterior + " surface

Median absolute deviation measurement distribution across 721 slices of exterior surface

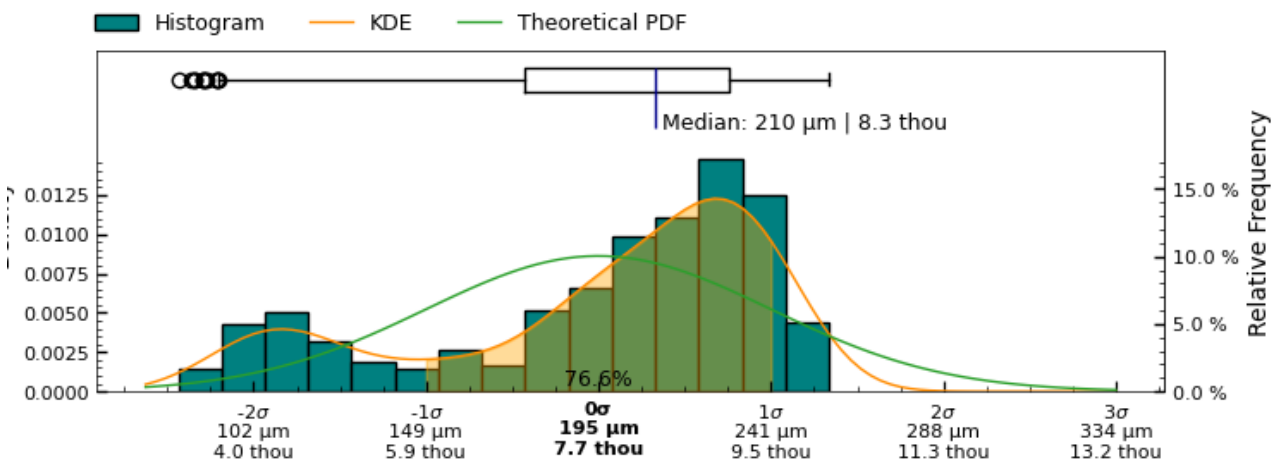


Figure 15: Median absolute deviation measurement distribution across measured slices of exterior surface

Circularity analysis of interior surface

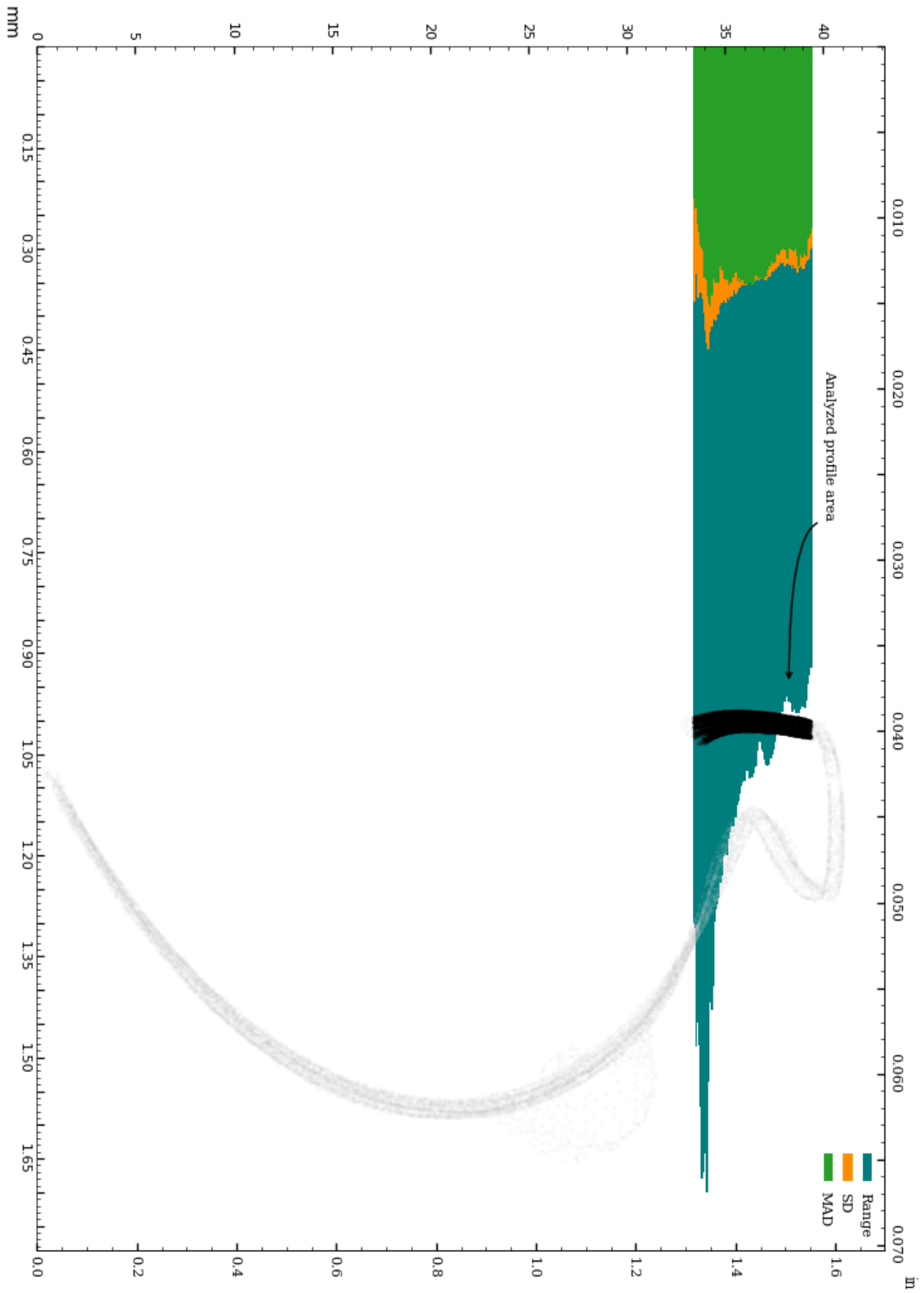


Figure 16: Circularity of interior surface.

Circularity analysis of interior surface, Standard Deviation and Median Absolute Deviation

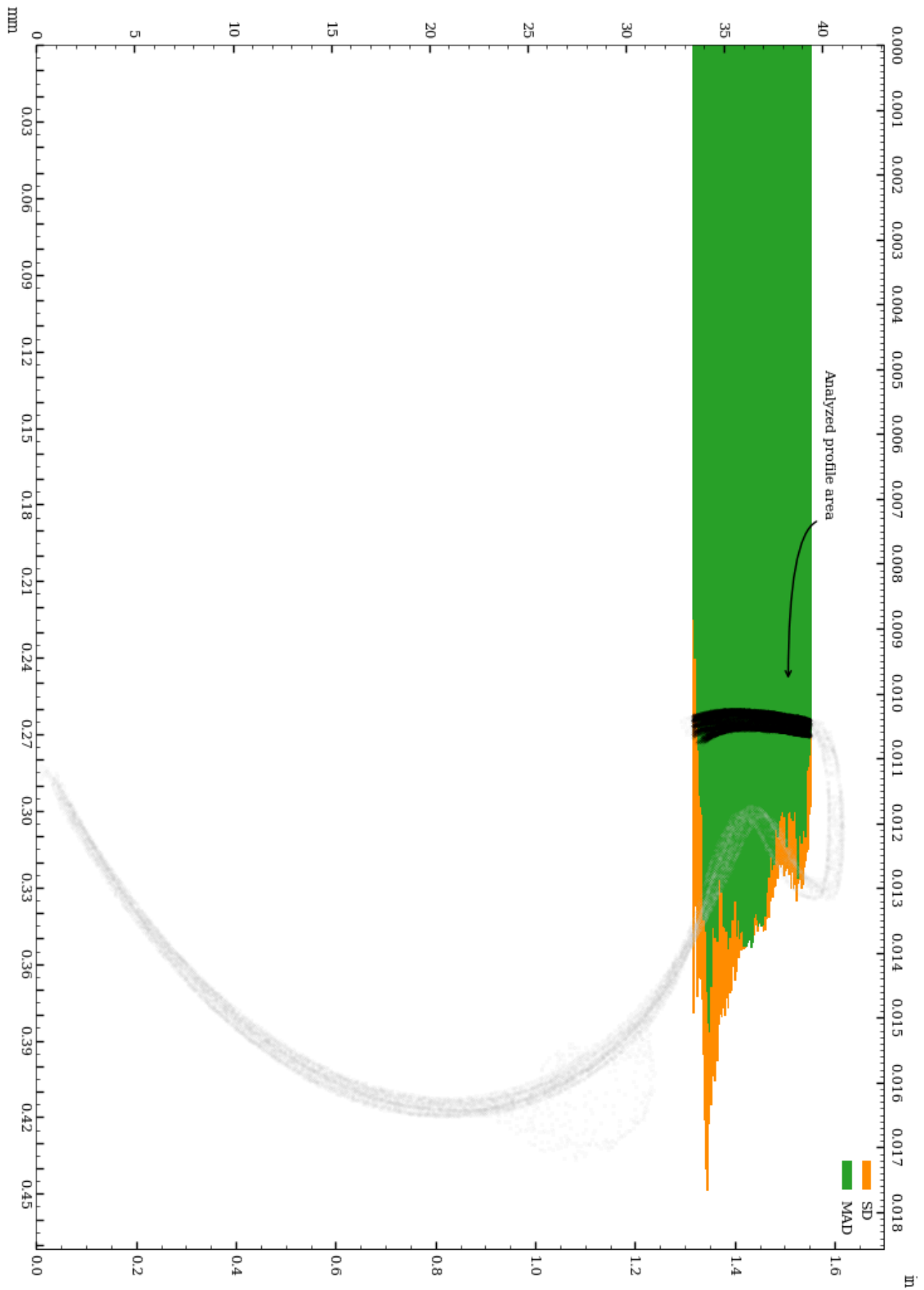


Figure 17: Vessel circularity of interior surface, standard deviation and median absolute deviation.

The distributions of the circularity measurements across 120 slices of the interior surface are shown below.

Range measurement distribution across 120 slices of interior surface

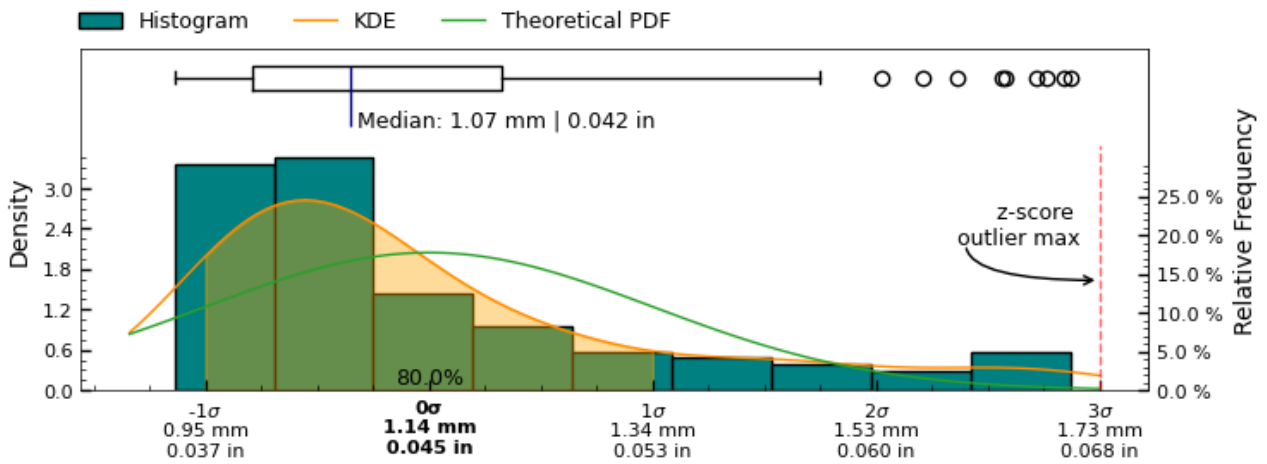


Figure 18: Range measurement distribution across measured slices of interior surface

Standard deviation measurement distribution across 120 slices of interior surface

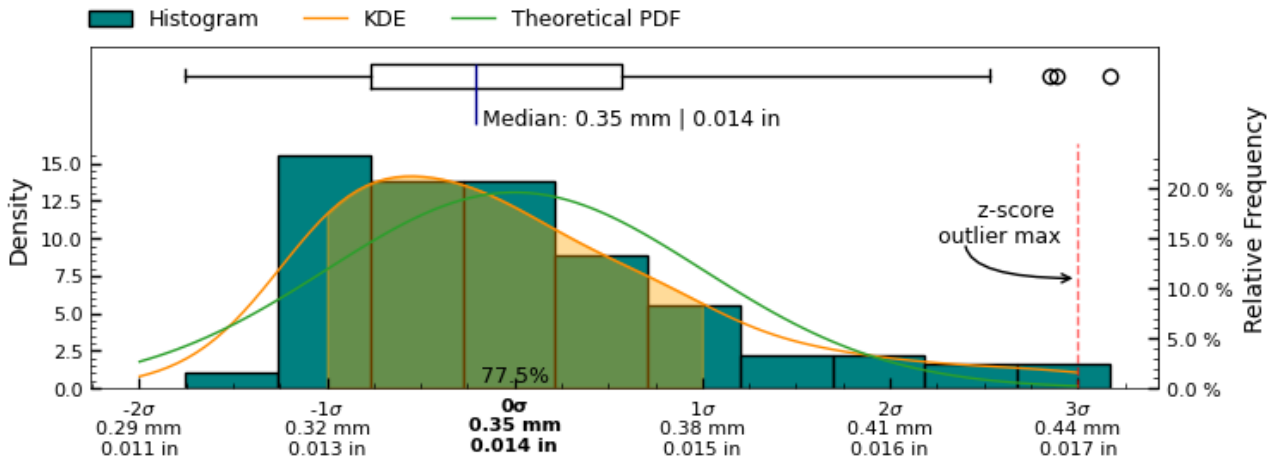


Figure 19: Standard deviation measurement distribution across measured slices of " + interior + " surface

Median absolute deviation measurement distribution across 120 slices of interior surface

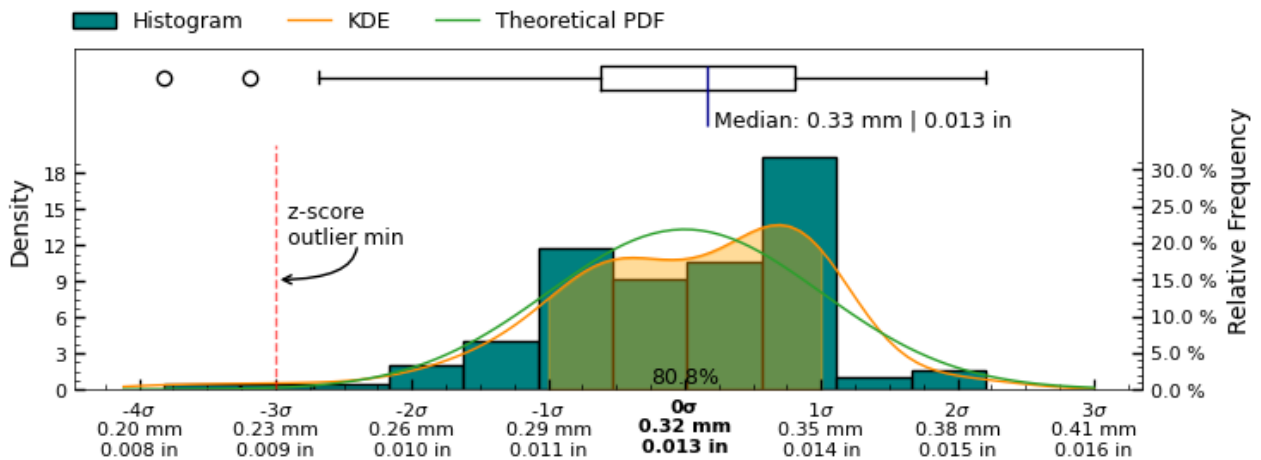


Figure 20: Median absolute deviation measurement distribution across measured slices of interior surface

Concentricity

The concentricity metric describes the deviation in the center-point of the referenced features. As such, it is a measure to determine if several features of the object share the same center point/axis, and how closely. See Figure 21 for a visual representation of this metric.

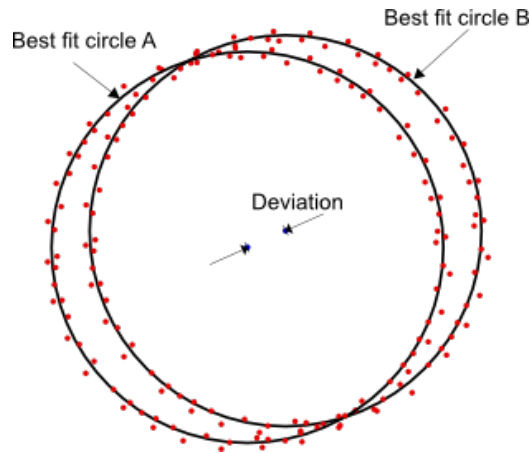


Figure 21: Concentricity measures the deviation (distance) between the center of two circles.

Determination of concentricity has been carried out by establishing the best fit circles of sample slices, using RANSAC (Random sample consensus) algorithm for outlier detection of a least squares circle regression on the scanned data-points at each cross-section, to estimate centers of each cross-section.

The concentricity between both the interior and exterior circular cross-sections is explored for cross-section measurements with the same Z-coordinates.

Additionally, the concentricity between each cross-section measurement defined in Figure 4 and the datum axis $(x, y) = (0, 0)$ has been calculated to establish the deviation of the feature center from the datum axis.

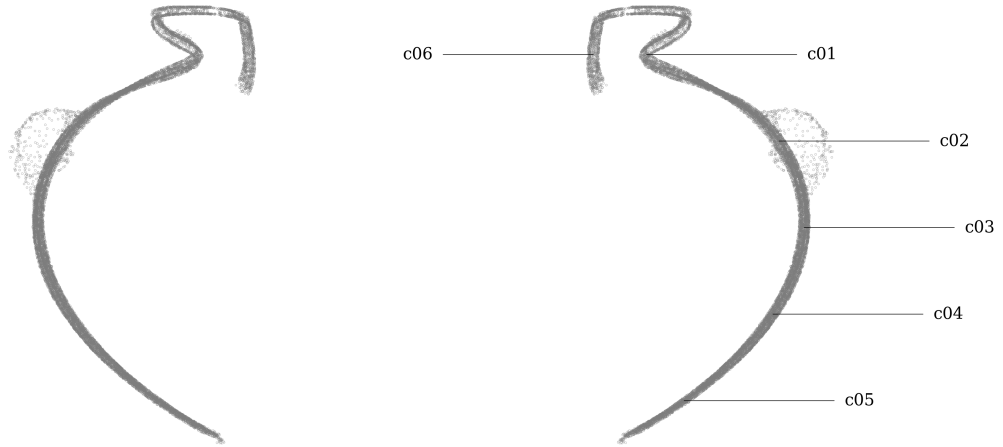


Figure 22: Concentricity measurement sample location on MV018.

Metric

Tag	Reference	Deviation	Sample size	Circle fit residuals analysis for sample listed in Tag column						
				Range full	Range inliers	SD full	SD inliers	MAD full	MAD inliers	Center (x,y)
		mm		mm	mm	mm	mm	mm	mm	μm
c01	z-axis	0.166	1487	1.074	1.074	0.335	0.335	0.251	0.251	-166, -17
c02	z-axis	0.117	1305	1.089	1.089	0.293	0.293	0.209	0.209	-4, -117
c03	z-axis	0.017	2078	1.000	1.000	0.282	0.282	0.247	0.247	-7, 16
c04	z-axis	0.012	1641	0.924	0.924	0.272	0.272	0.240	0.240	11, -5
c05	z-axis	0.087	850	0.706	0.629	0.147	0.146	0.096	0.096	-71, 51
c06	z-axis	0.487	942	1.070	1.070	0.349	0.350	0.348	0.355	-419, 248
c01	c06	0.366	1487	1.074	1.074	0.335	0.335	0.251	0.251	254, -265

Imperial

Tag	Reference	Deviation	Sample size	Circle fit residuals analysis for sample listed in Tag column						
				Range full	Range inliers	SD full	SD inliers	MAD full	MAD inliers	Center (x,y)
		in		in	in	in	in	in	in	thou
c01	z-axis	0.0066	1487	0.0423	0.0423	0.0132	0.0132	0.0099	0.0099	-6.5, -0.7
c02	z-axis	0.0046	1305	0.0429	0.0429	0.0115	0.0115	0.0082	0.0082	-0.1, -4.6
c03	z-axis	0.0007	2078	0.0394	0.0394	0.0111	0.0111	0.0097	0.0097	-0.3, 0.6
c04	z-axis	0.0005	1641	0.0364	0.0364	0.0107	0.0107	0.0095	0.0095	0.4, -0.2
c05	z-axis	0.0034	850	0.0278	0.0248	0.0058	0.0058	0.0038	0.0038	-2.8, 2.0
c06	z-axis	0.0192	942	0.0421	0.0421	0.0137	0.0138	0.0137	0.0140	-16.5, 9.8
c01	c06	0.0144	1487	0.0423	0.0423	0.0132	0.0132	0.0099	0.0099	10.0, -10.4

Table 3: Concentricity analysis of MV018.

Concentricity analysis of c01

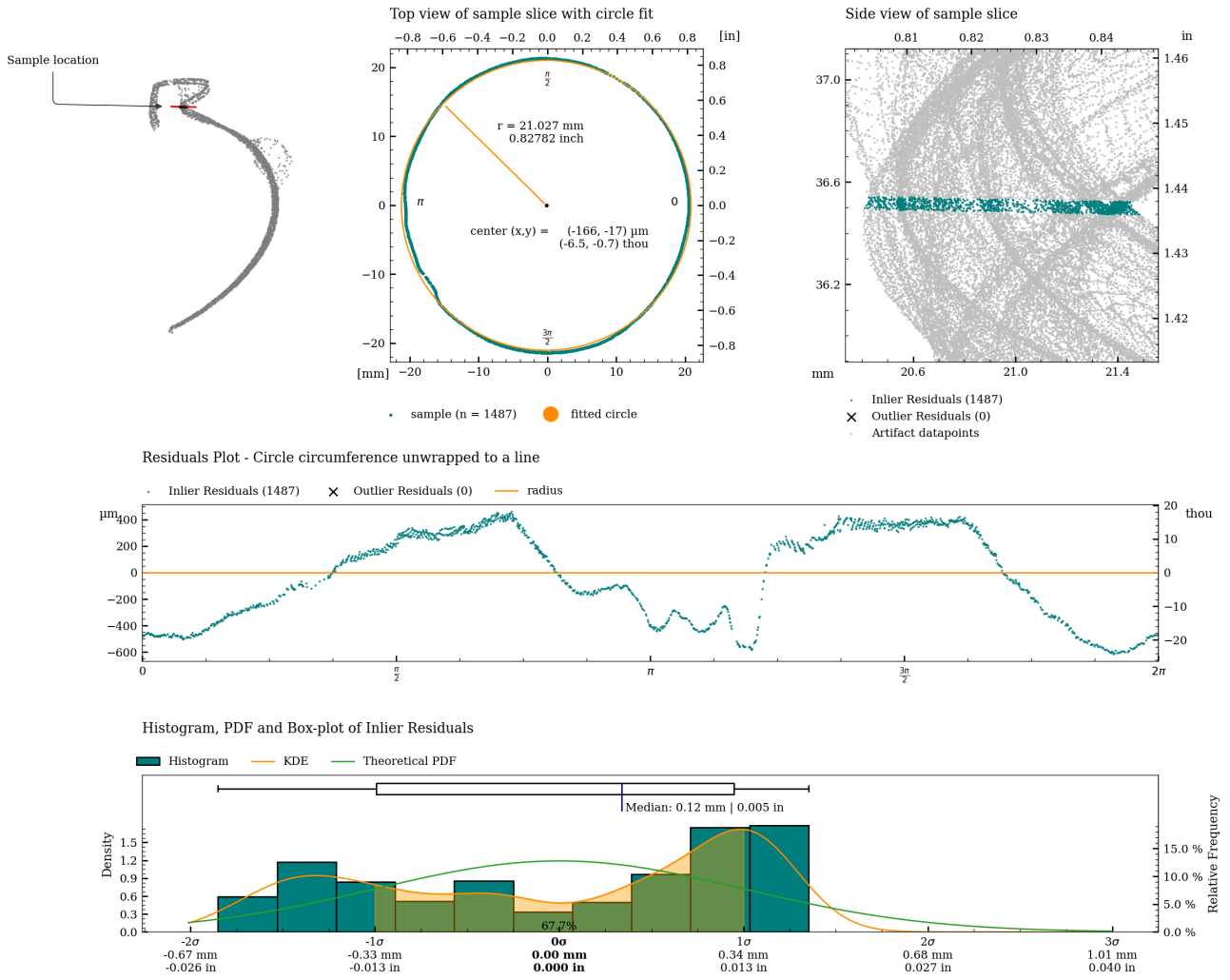


Figure 23: Detailed plot of concentricity measurement for c01.

Concentricity analysis of c02

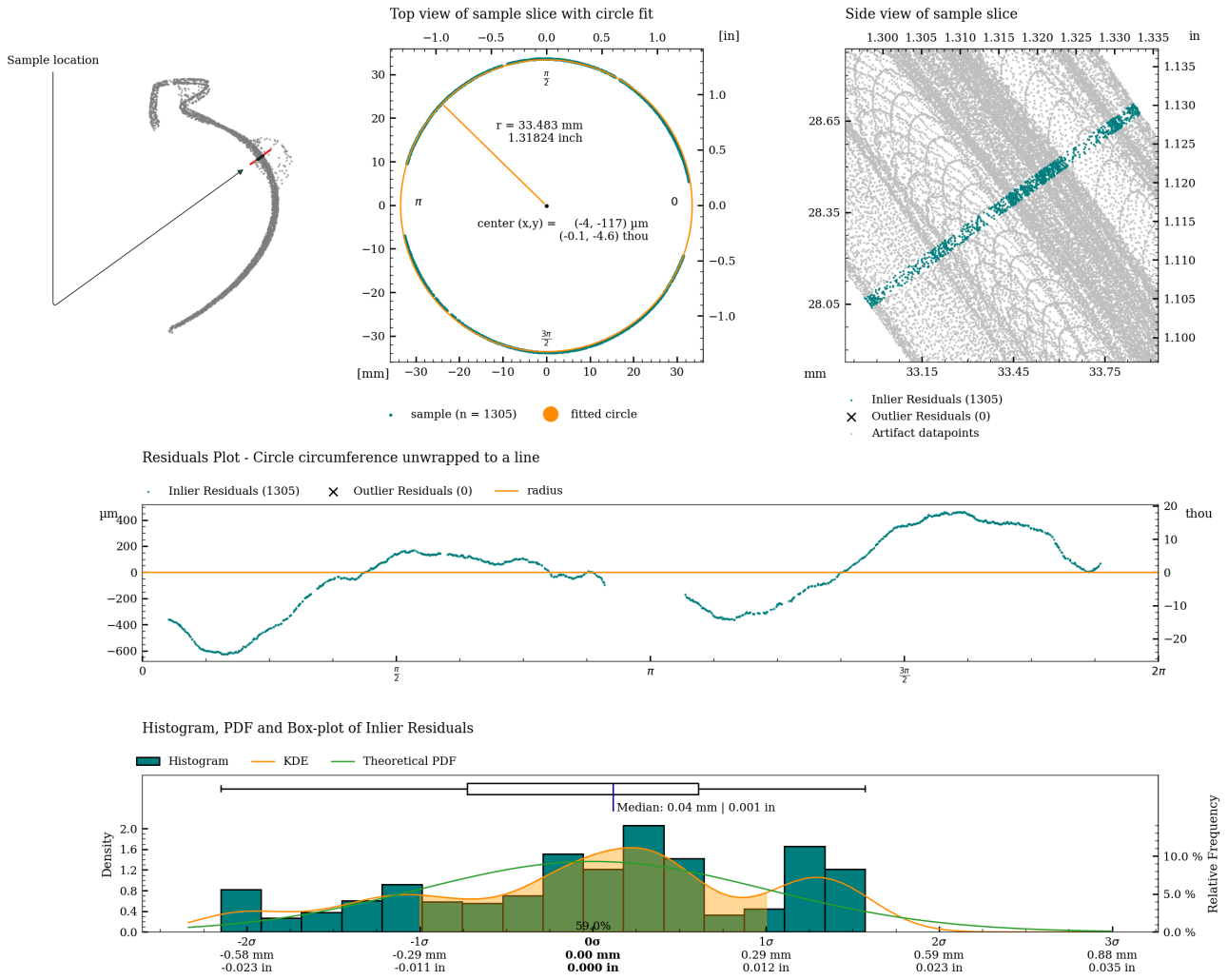


Figure 24: Detailed plot of concentricity measurement for c02.

Concentricity analysis of c03

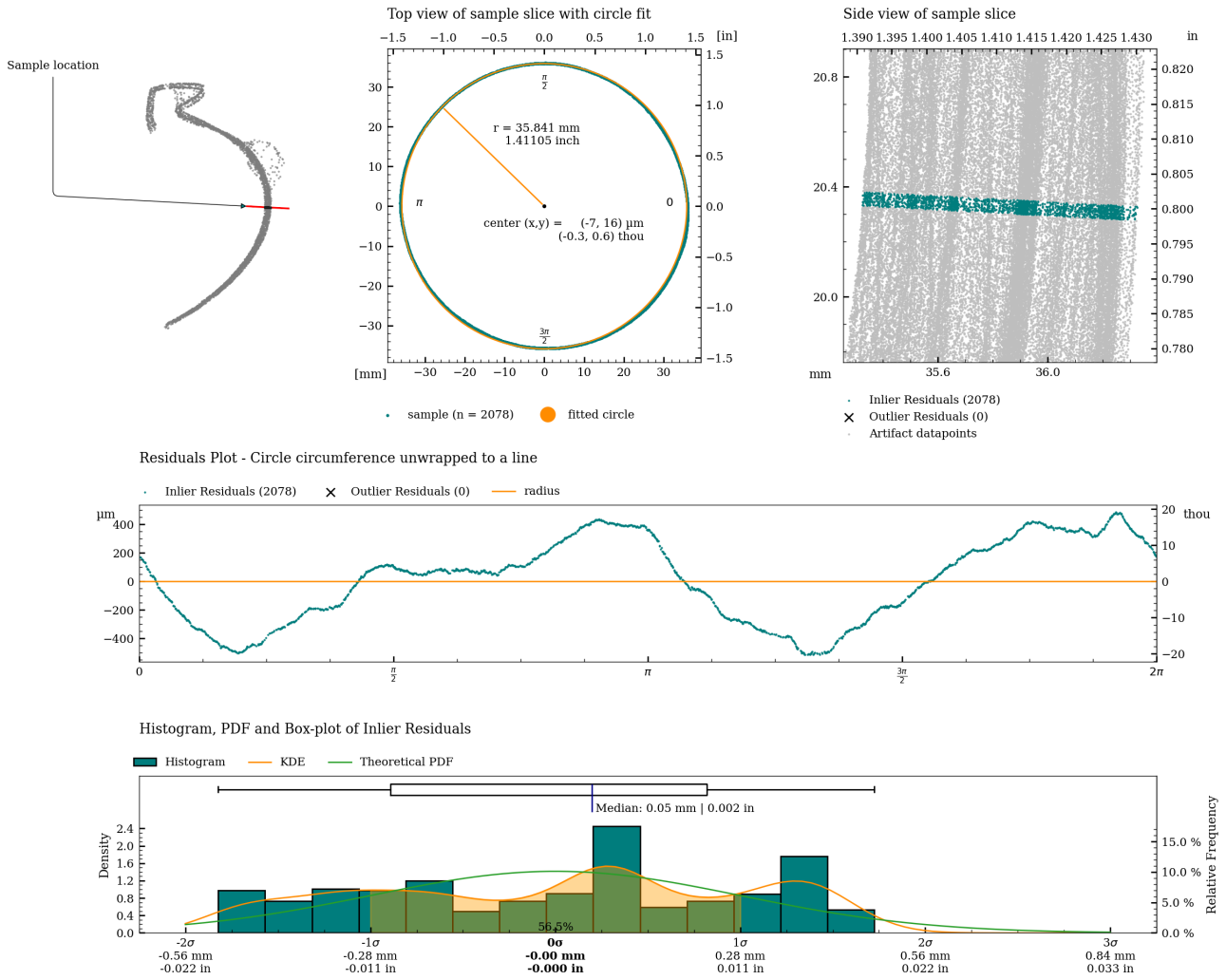


Figure 25: Detailed plot of concentricity measurement for c03.

Concentricity analysis of c04

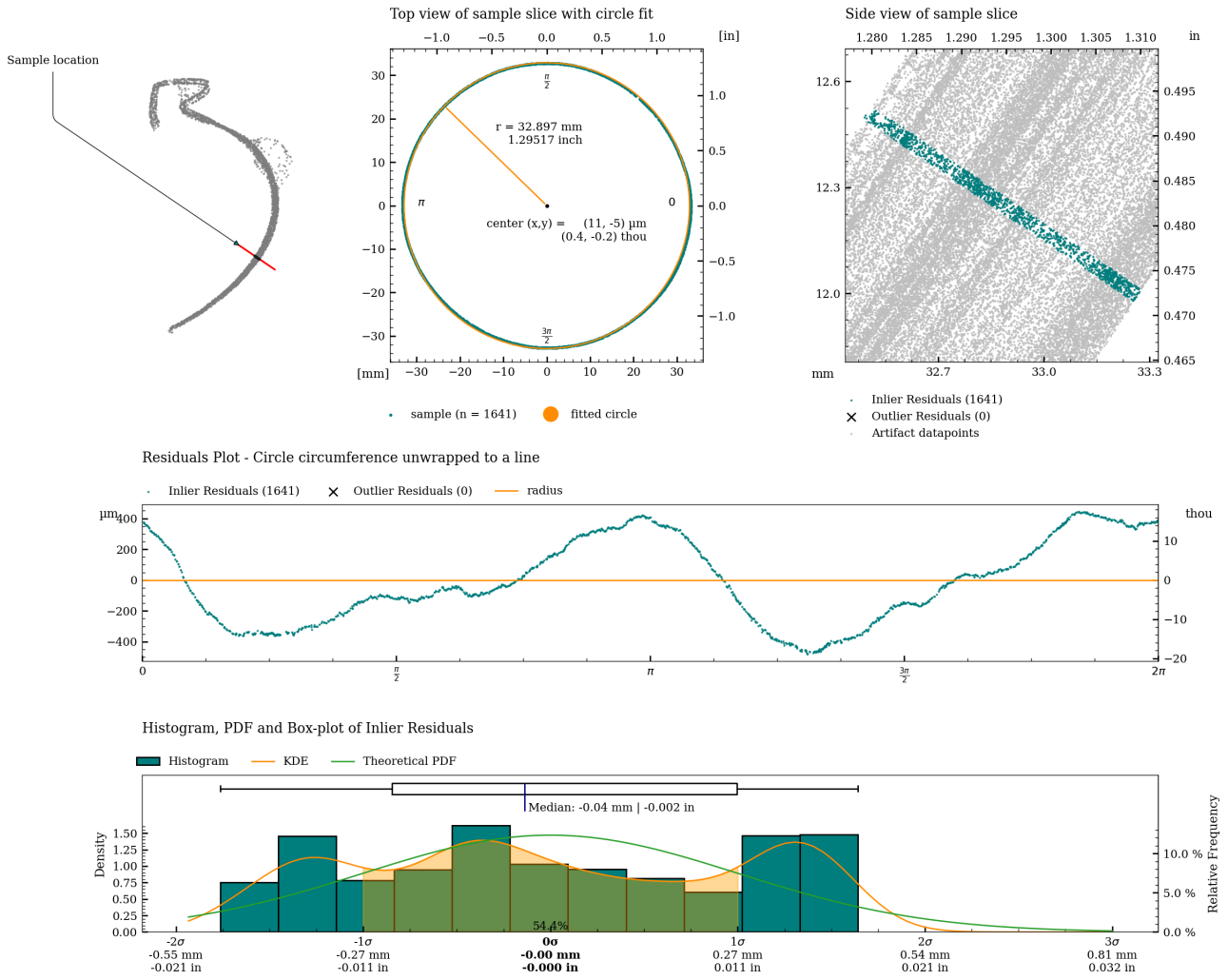


Figure 26: Detailed plot of concentricity measurement for c04.

Concentricity analysis of c05

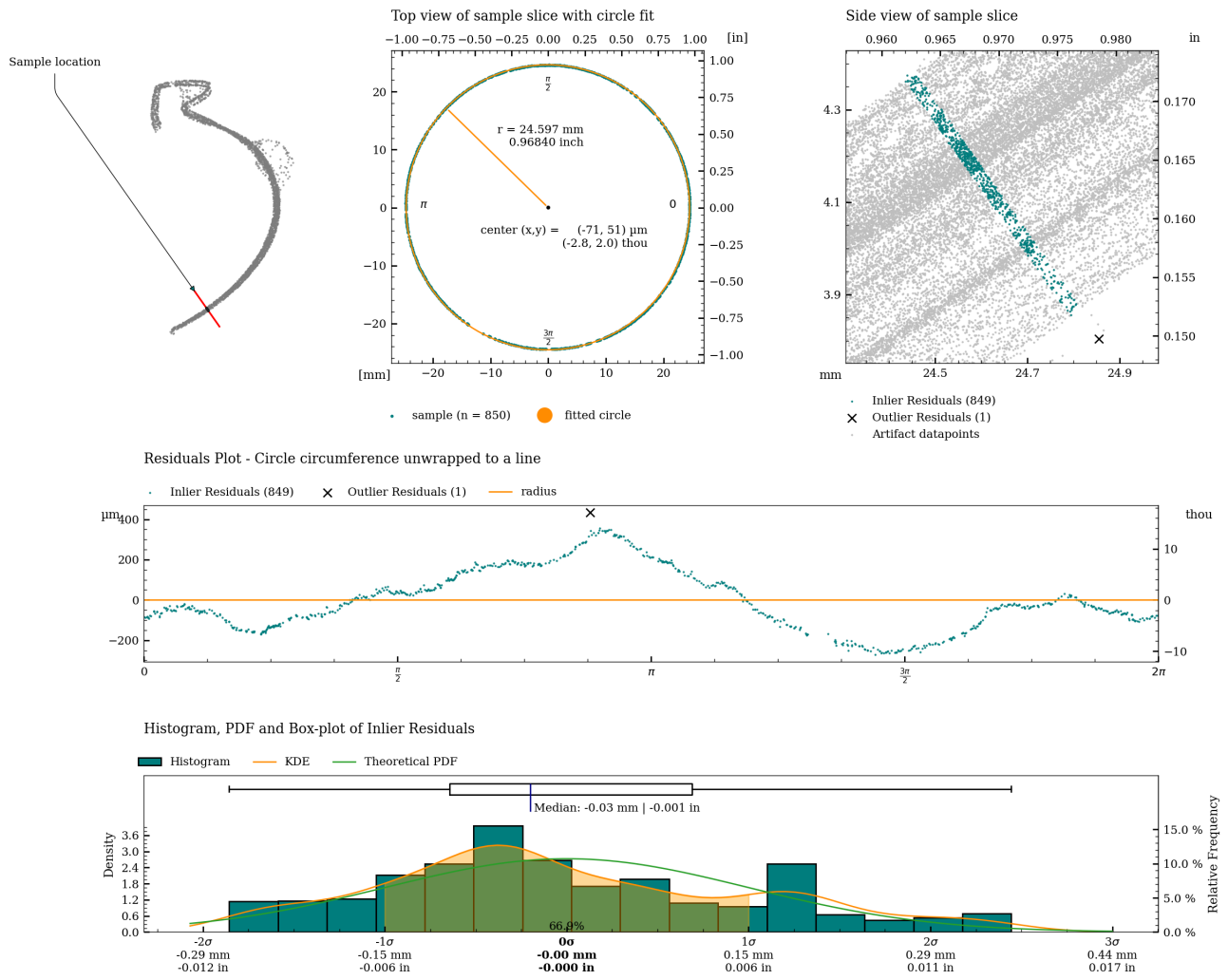


Figure 27: Detailed plot of concentricity measurement for c05.

Concentricity analysis of c06

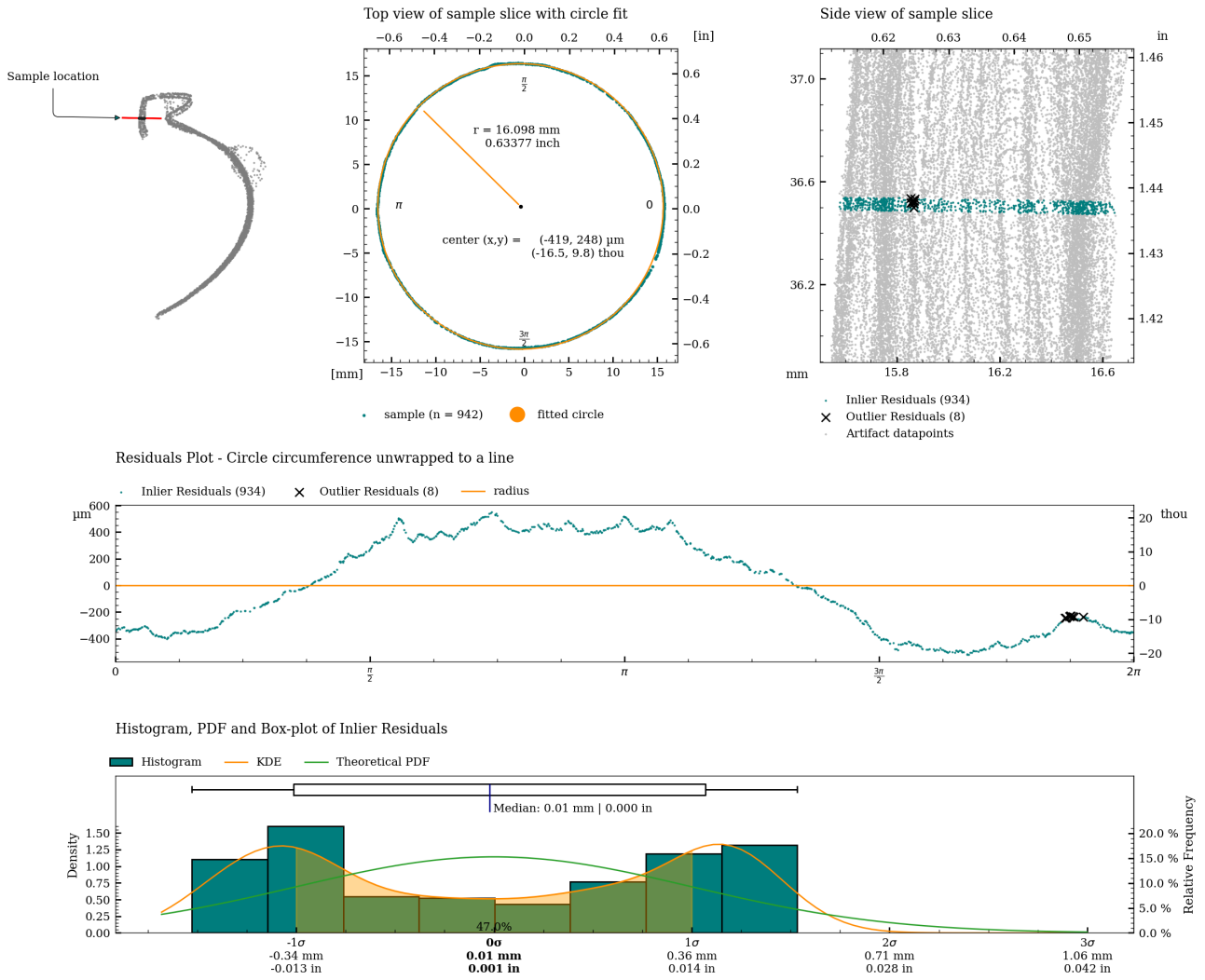


Figure 28: Detailed plot of concentricity measurement for c06.

Coaxiality

Coaxiality is a measure of the deviation in the central axis of an object. Coaxiality measurements are calculated using RANSAC (Random sample consensus) algorithm for outlier detection of a least squares circle regression on cross-sections of the vessel (excluding potential handles) to estimate the best fit circle centers for each slice of the vessel.

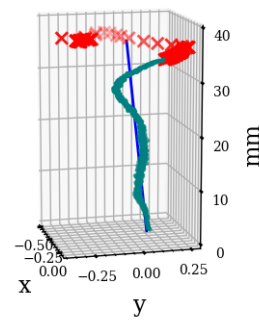
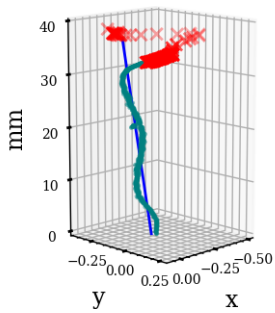
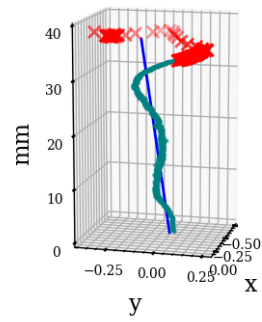
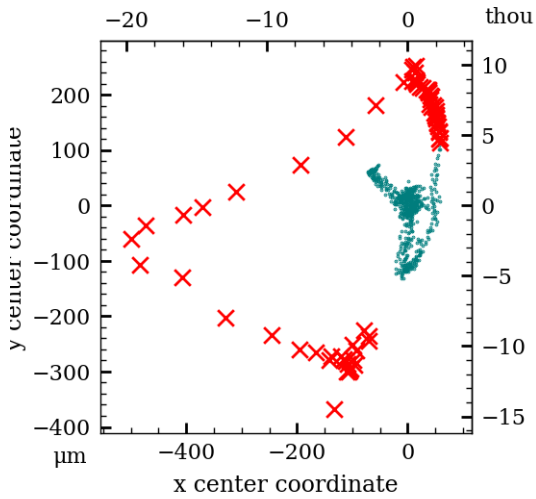
Coaxiality is measured for:

- The exterior surface (excluding handles)
- The interior surface

	Exterior		Interior	
Analyzed Slices			721	120
Median sample size			1341	964
Slice Height	50 μm	2.0 thou	50 μm	2.0 thou
Statistics with Z-axis as Reference				
Median Absolute Deviation (MAD)	44 μm	1.7 thou	494 μm	19.5 thou
Standard Deviation (SD)	75 μm	2.9 thou	52 μm	2.0 thou
Root Mean Square Deviation (RMSD)	101 μm	4.0 thou	504 μm	19.8 thou
Statistics with Best Fit Central Axis as Reference				
Best fit Central Axis Equation (in metric coordinate system with unit [mm])	$x = -0.042 + t-0.00213$ $y = 0.057 + t0.00352$ $z = 0.000 + t-0.99999$		$x = -0.434 + t-0.00074$ $y = 1.671 + t0.03815$ $z = 0.000 + t-0.99927$	
Axis tilt		-0.121°		-0.041°
Median Absolute Deviation (MAD)	34 μm	1.4 thou	27 μm	1.1 thou
Standard Deviation (SD)	79 μm	3.1 thou	22 μm	0.9 thou
Root Mean Square Deviation (RMSD)	100 μm	3.9 thou	37 μm	1.5 thou

Table 4: Coaxiality analysis of vessel MV018.

Coaxiality plots, exterior surface



Coaxiality residuals from fitted axis, exterior surface

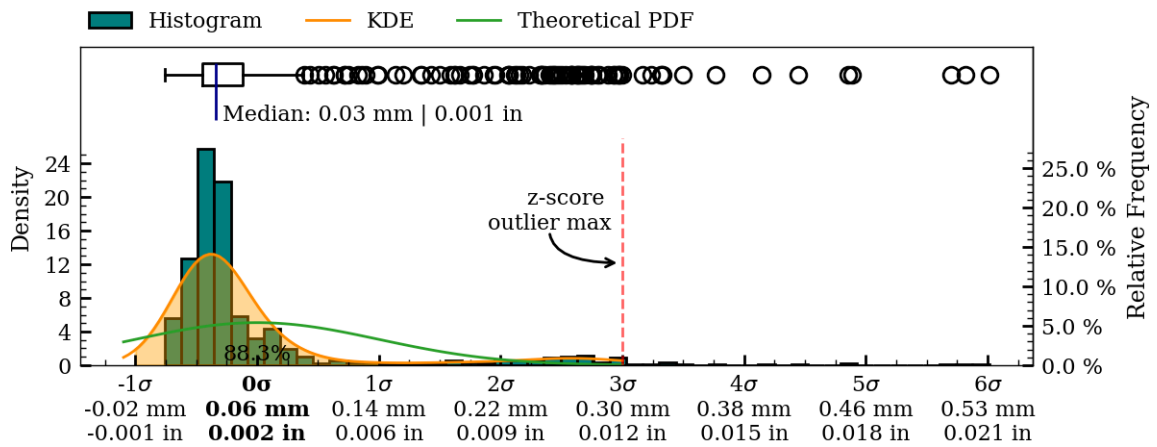
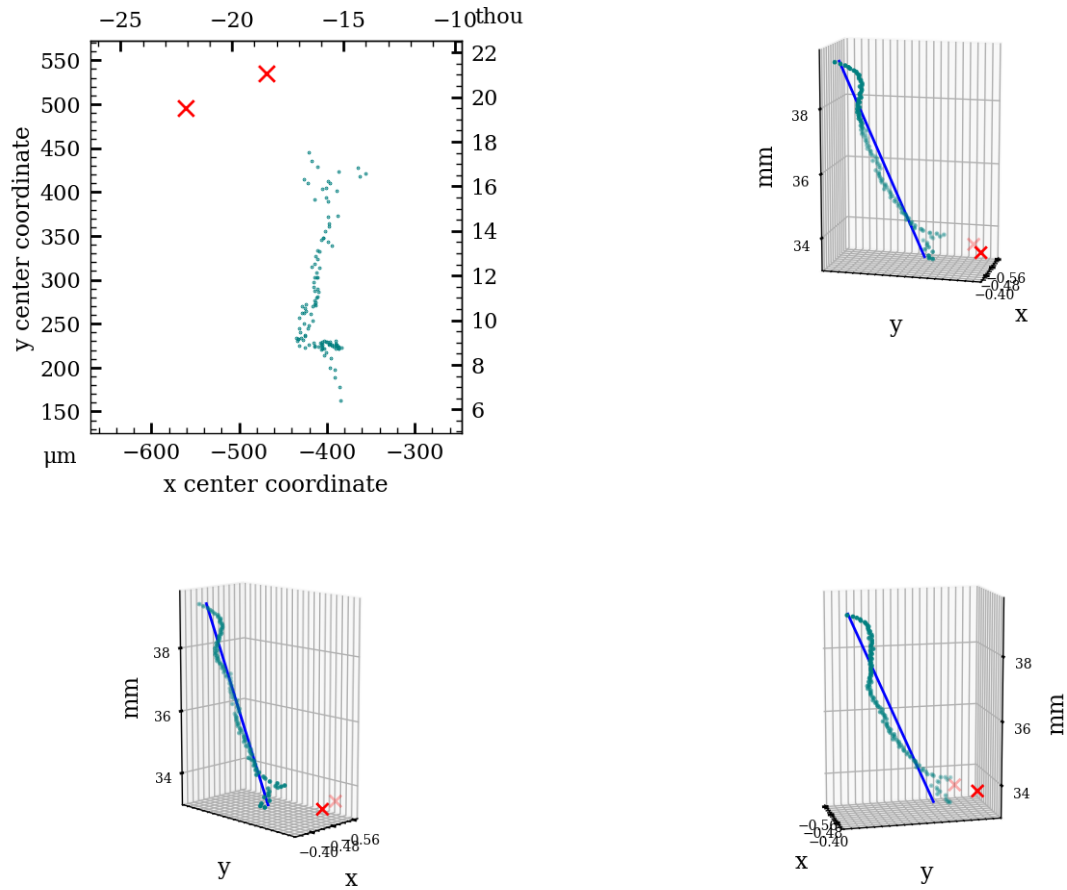


Figure 29: Coaxiality residual plots of exterior surface, MV018.

Coaxiality plots, interior surface



Coaxiality residuals from fitted axis, interior surface

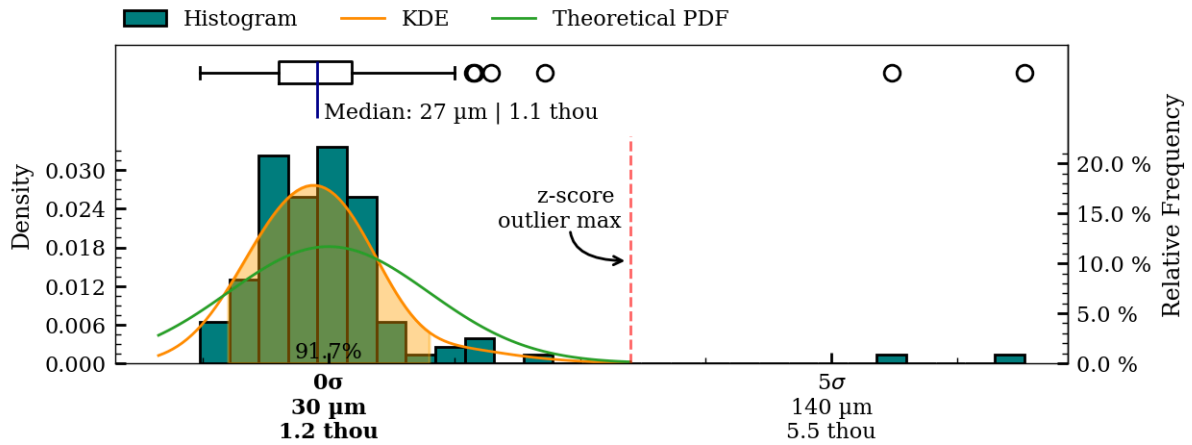


Figure 30: Coaxiality residual plots of interior surface, MV018.

Surface Variability

To illustrate the overall surface deviations of the object, a surface variability heatmap has been created. This heatmap provides an accessible overview of the topography of the manufacturing precision and surface structure of the object.

The raw scan files from FreeScan Combo+ often produce geometry artifacts on the surface of the scanned object. If present these will be clearly seen, as falling outside of the heatmap range, and as such being uncolored. These geometry artifact, if present, will and increase the total range of the surface deviation statistics.

The surface variability measurements are created by fitting a number of higher-order polynomials to the two-dimensional folded profile of the scan data. This process creates an idealized mathematical representation of actual surface curvature of object, and as such provides a continuous model representation of the actual object. It is important to note that only such a non-discretized representation is sufficient to avoid introducing inconsistently varying errors in the mapping of the final surface deviation results, that the rendered heatmaps are based on.

To produce the final surface variability map, the distance from each scanned vertex to the fitted polynomial is calculated and used as the mapping function input, for applying colours to the surface of the object.

It is important to note that this variability map does not describe deviations from the original *intended* shape of the artifact (if any), as this shape (the *intended design*, so to speak) will have been lost to time. It does however provide a very informative visualization of the texture and structure of the surface and very importantly, *does* highlight potential manufacturing-relevant patterns in the surface texture (if present). Such patterns are, as an example, clearly evident on the interior surface of artifact PV001.

Exterior surface

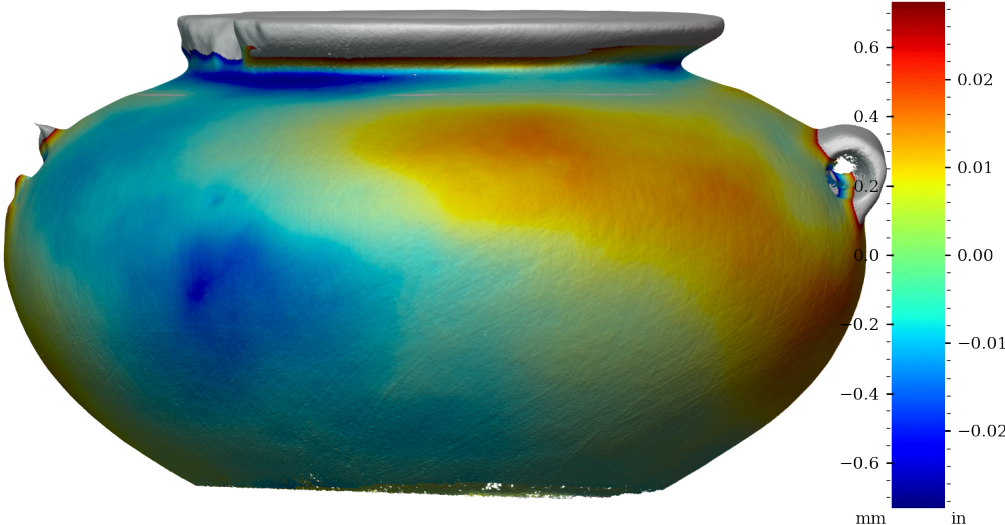


Figure 31: Surface variability heatmap of MV018, front view

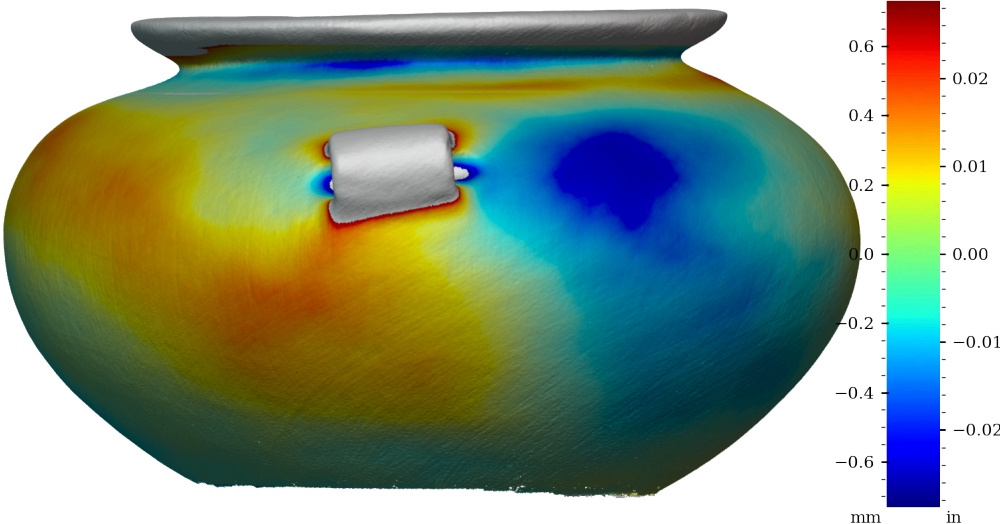


Figure 32: Surface variability heatmap of MV018, rotated 90°

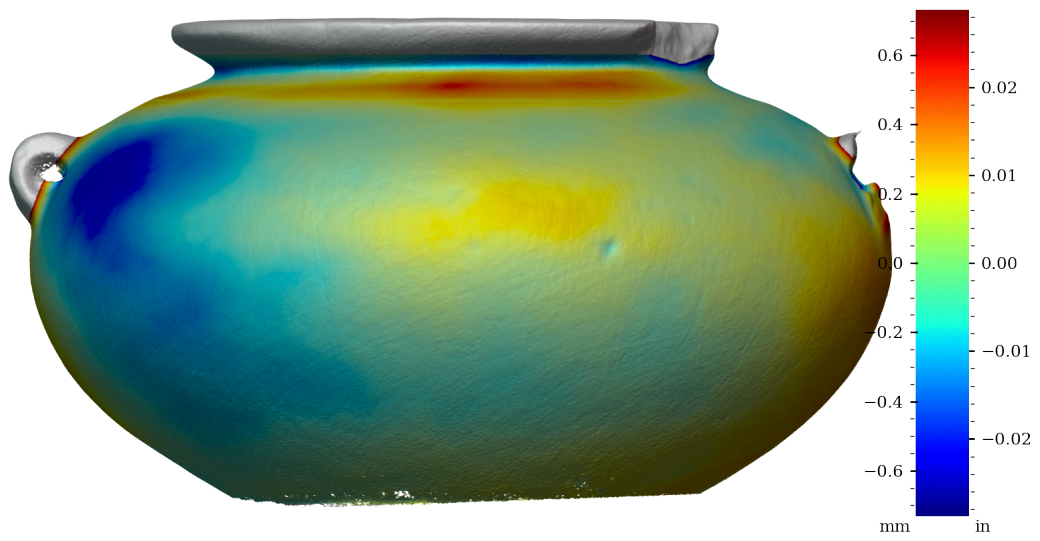


Figure 33: Surface variability heatmap of MV018, rotated 180°

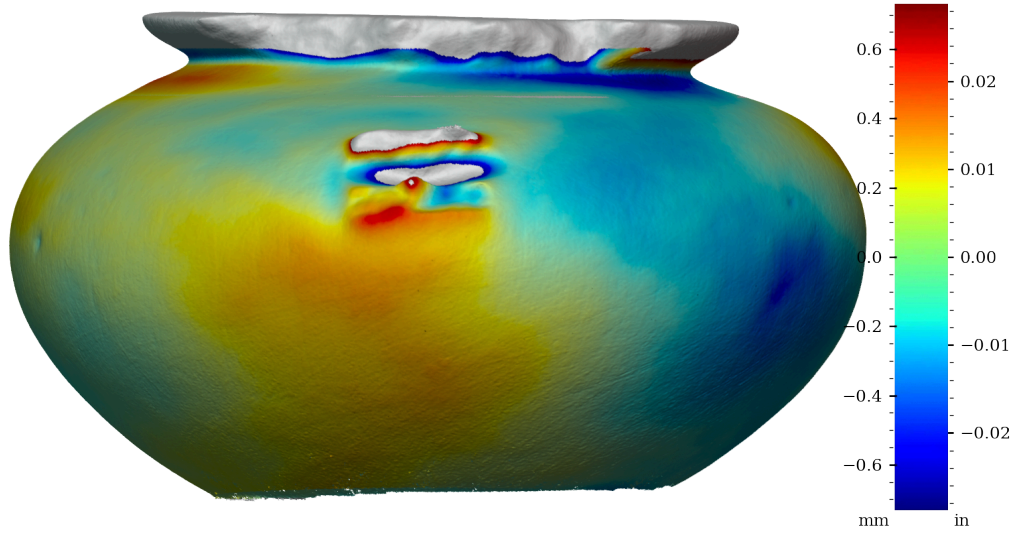


Figure 34: Surface variability heatmap of MV018, rotated 270°

Interior surface

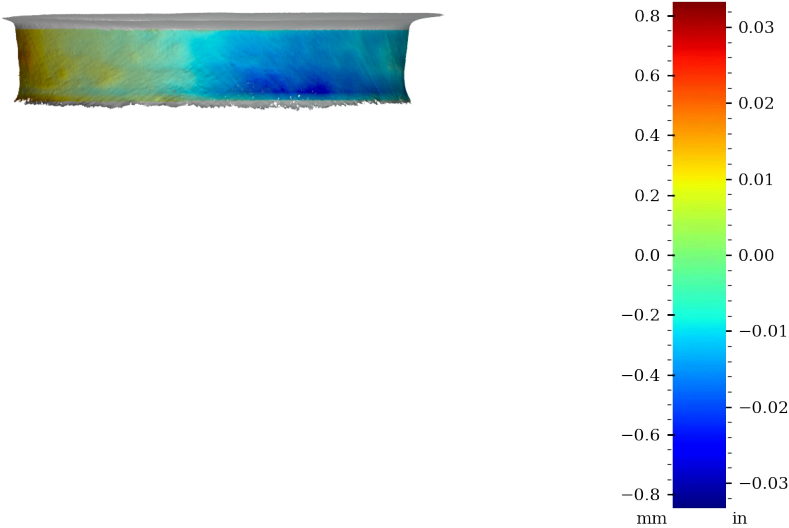


Figure 35: Surface variability heatmap of MV018, front view

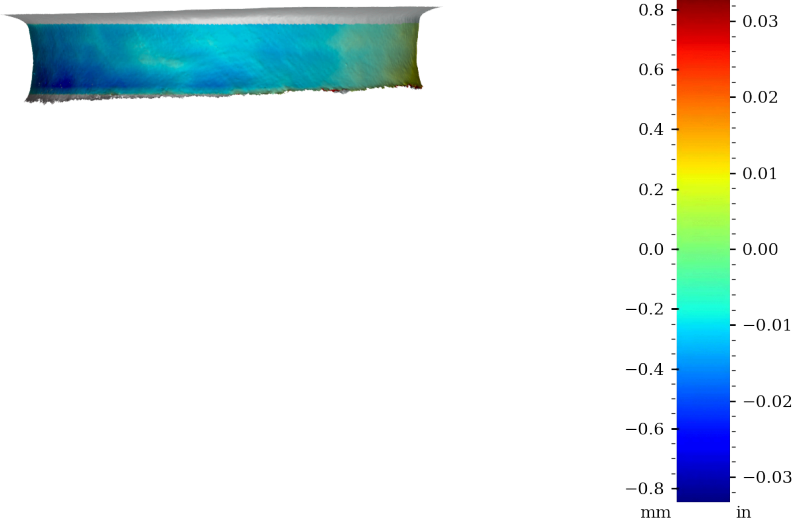


Figure 36: Surface variability heatmap of MV018, rotated 90°

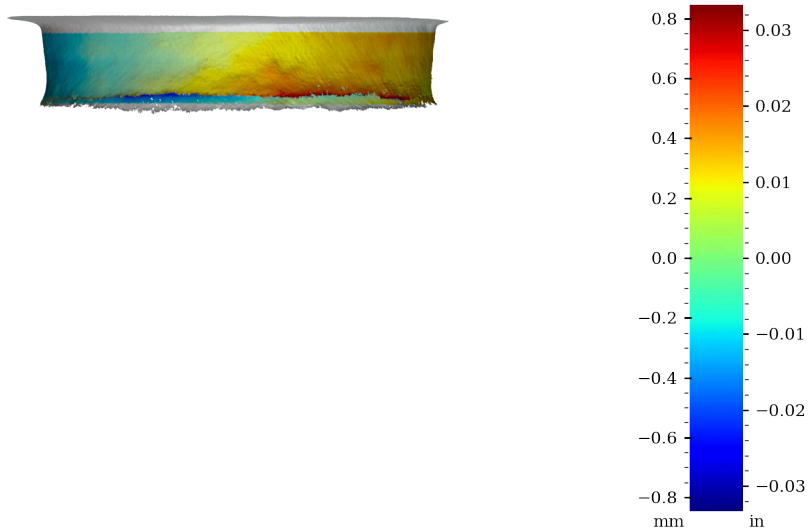


Figure 37: Surface variability heatmap of MV018, rotated 180°

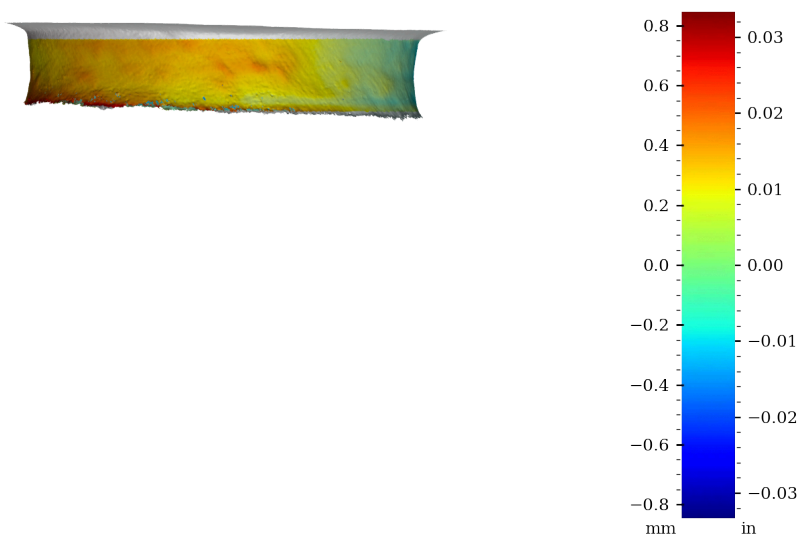


Figure 38: Surface variability heatmap of MV018, rotated 270°

Surface variability statistics

Area	MSD	RMSD	SD	Mean AD	Median AD	Range	Min	Max	Sample size
	mm ²	mm	mm	mm	mm	mm	mm	mm	
Exterior	0.0840	0.290	0.290	0.188	0.218	3.550	-0.736	2.814	1665759
Interior	0.1244	0.353	0.353	0.324	0.314	1.730	-0.684	1.046	114304
	in ²	in	in	in	in	in	in	in	
Exterior	0.000130	0.0114	0.0114	0.0074	0.0086	0.1398	-0.0290	0.1108	1665759
Interior	0.000193	0.0139	0.0139	0.0127	0.0124	0.0681	-0.0269	0.0412	114304

Table 5: Surface variability statistics, MV018

Table 5 shows the statistics of the distance from the scan vertices to the best fit object model. These statistics are briefly explained below.

Mean Squared Deviation (MSD), also known as Mean Squared Error (MSE).

$$\text{MSD} = \frac{\sum_{i=1}^n (y_i - \hat{y})^2}{n}$$

The MSD metric shows the the average squared difference between the scanned points and the fitted composite polynomial model (a value of 0 would be a perfect match). This metric emphasizes imperfections in the surface of the artifact. Outliers will negatively influence this metric, raising the value of the MSE.

Root Mean Squared Deviation (RMSD), also known as Root Mean Squared Error (RMSE).

$$\text{RMSD} = \sqrt{\frac{\sum_{i=1}^n (y_i - \hat{y})^2}{n}}$$

Measures the dispersion of the measured surface variability y_i around a model predictor (\hat{y}). By obtaining the root of the MSD, the exponent will be removed from the measurement, enabling comparisons with other statistics of the same unit and making it more accessible to those familiar with the RMSD metric. This measure is used to assess the fit of a regression model to a dataset, in this case our best fit composite polynomial model. The lower the RMSD metric, the better the fit.

Standard Deviation (SD)

$$s = \sqrt{\frac{\sum_{i=1}^n (y_i - \bar{y})^2}{n - 1}}$$

Measures the dispersion of the measured surface variability y_i around the mean (\bar{y}). If the residuals are normally distributed around the mean ($\bar{y} \approx 0$), the SD will be equal to the RMSD. See Figure 39 and Figure 40

Mean Absolute Deviation (MeanAD)

$$\text{MeanAD} = \frac{\sum_{i=1}^n |y_i - \bar{y}|}{n}$$

This metric is similar to the SD, but the difference between the residuals and the mean is *not* squared. Instead of indicating the spread of the data, we look at the average distance between each data point and the mean. The Mean Absolute Deviation is affected less by outliers than the Standard Deviation.

Median Absolute Deviation (MedianAD)

$$\text{MedianAD} = \text{median}(|y_i - \text{median}(y)|)$$

The Median Absolute Deviation is measure of the dispersion of the data around the median.

Range

$$\max(y_i) - \min(y_i)$$

Range is a measure of the total spread of the residuals

Histogram, KDE and Box-plot of measured surface variability - exterior surface

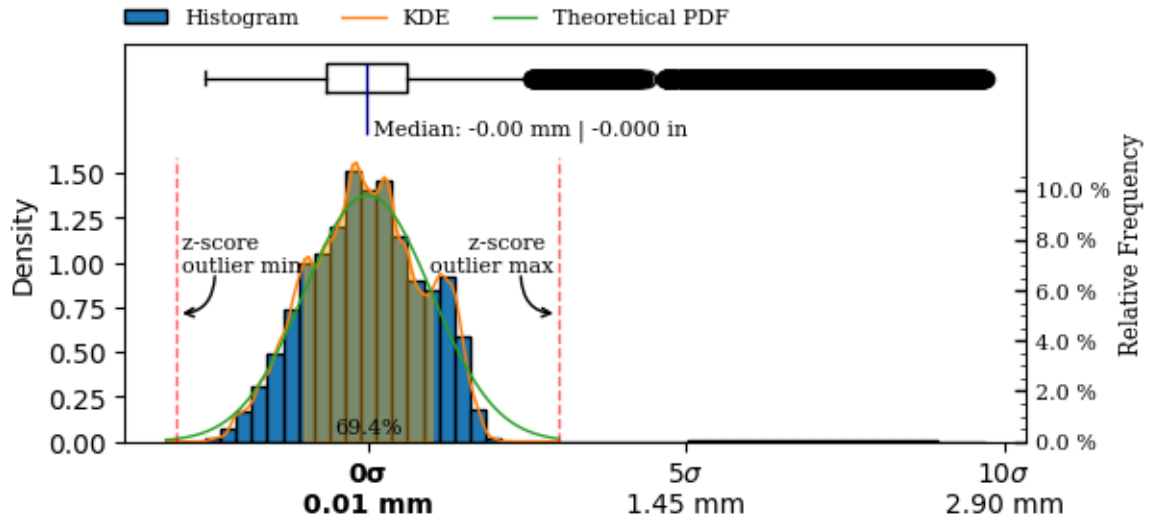


Figure 39: Exterior surface variability boxplot, kds and histogram.

Histogram, KDE and Box-plot of measured surface variability - interior surface

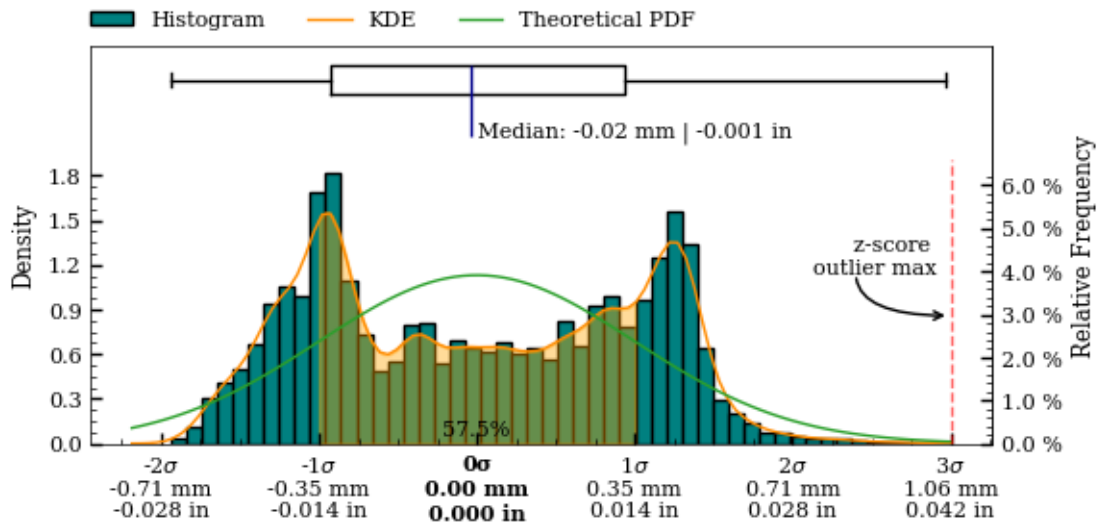


Figure 40: Interior surface variability boxplot, kds and histogram.

Precision Score Of The Artifact

To enable valid comparison of the manufacturing precision of different artifacts, a metric that robustly quantifies the overall precision of the object is required. The considerations for such a metric will be explored in this section.

Based on these considerations, a *Precision Score* metric will be defined.

For an object to be described as having been manufactured with high precision, several qualities must be present *concurrently*, and throughout the *entire* geometry of the final object. A given object may exhibit high levels of one or more *components* of precision, but be lacking in others. For example:

- An object may present high levels of coaxiality, but lack circularity.
- An object may exhibit good circularity, but show imperfections in the surface structure.
- An object may be smoothed to perfection *without* any circularity or coaxiality.
- An object may exhibit high levels of all of the above metrics in *some* areas, but not in others.

Therefore, a precision score metric **must** account for *all* aspects of the individual, underlying precision metrics (circularity, concentricity, coaxiality and surface variability) throughout the *entire* surface area of the object.

The composite high order polynomial model, used to generate the surface variability map (described in Surface Variability, p. 33) is the best continuous mathematical representation of the object available to us (lacking any original design plans, as would normally be available in metrological analysis). This idealized model encompasses all of the above component metrics.

In the creation of the model, all scan data-points are taken into account (excluding areas with extensive damage), making it the best possible idealized representation we can achieve. When this model has been accurately created, the deviation between the model and the scanned data-points can be calculated over the non-discretized polynomials, *without* the need for an “original” CAD model (and importantly, unless such a CAD model *actually* corresponded to the original design intent, it would be an insufficient comparison basis).

Within the context of defining a valid, overall precision metric, this approach satisfies the incorporation of all of the necessary metrics:

- **Circularity:** Because the reconstructed polynomial model is revolved around the Z-plane, the idealized representation is perfectly circular, and thus incorporates the circularity component.
- **Concentricity and coaxiality:** Because the Z-axis (datum axis) is the center axis of the model, it incorporates the concentricity and coaxiality components.
- **Surface variability:** Because the model is continuous and non-discretized, it can be used accurately for all points of the scan data, and incorporates the surface variability component.

The level of precision ultimately achieved in a physical object does not share a linear relationship with its manufacturing requirements. Since continuously higher levels of final precision becomes progressively harder to achieve, an overall precision metric must take this relationship into account.

A robust statistical metric that satisfies this requirement is the *Mean Squared Deviation* (MSD or MSE). Here specifically, we can utilize the mean square of the deviations between the model (\hat{y}) and the data-points (y_i).

Combining all of the above considerations, we can express a well-defined *Precision Score* metric, that provides an immediately accessible way to understand the overall precision of an object, while being statistically valid. Since the Mean Squared Deviation tends towards zero as the overall precision increases, the inverse of the Mean Squared Deviation is taken to obtain a precision score metric that increases as precision increases¹²:

$$\text{Precision Score} = \frac{n}{\sum_{i=1}^n (y_i - \hat{y})^2}$$

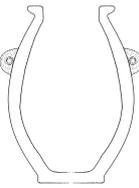
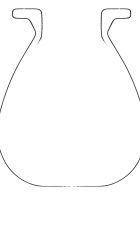
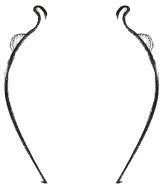
¹²The precision score unit is $\frac{1}{\text{mm}^2}$

A precision score will be calculated separately for:

- The exterior surface
- The interior surface
- The full surface

As most scans do not include sufficient scan data for the interior surface, the exterior surface will be used for calculating the precision score in most cases. In the rare case that the scan data is more complete for the *interior* surface, this will be used instead.

Table 6 shows the precision score of this artifact (MV018), compared to the two most precise, and the two least precise vessels currently analyzed.

Artifact		Material	Precision Score	Link to Report
		PV001 Red Granite	1905 Full: 980 Exterior: 1905 Interior: 705	Report Publication
		PV006 Dark grey granite	621 Full: 521 Exterior: 621 Interior: 152	Report Publication
		MV018 Diorite	12 Full: 12 Exterior: 12 Interior: 8	Report Publication
		MV001 Pottery	1.93 Full: 1.92 Exterior: 1.93 Interior: 1.85	Report Publication
		MV010 Calcite (Egyptian Al-abaster)	1.12 Full: 0.64 Exterior: 1.12 Interior: 0.20	Report Publication

Analysis Roadmap

While the current iteration of this work already provides valuable results, continued future additions and improvements will enhance their utility further. This section details planned iterative updates and improvements, to both the reports themselves, and to the underlying methodology and software they are created with.

Alignment Section

- Detailed exploration of different circle regression algorithms
- If handles are present on the vessel, exploring alignment of the vessels so the handle positions match each other
- Add optimization of the perpendicular surface deviation, with the best results of the coaxial alignment
- Align by minimizing circularity results (of rotated sample slice, to compensate for sample height distortions)

Measurements of Precision

- Section detailing how measurements perpendicular to the surface curvature are obtained
- Detailed surface area analysis, exploring the residual patterns throughout subsequent sample slices of the artifact surface
- Wall thickness deviation color map
- Robust outlier identification on circularity, to better handle analysis of damaged areas of the artifacts in addition to removal of interior crystalline structure points present in CT scans
- Layout updates to the charts and tables

Visibility of Outliers and Damaged Sections

- Identification and marking of damaged parts
- Visualization of outliers on the artifact surface

Exploration of Mathematical Primitives

- Analysis of selected curvatures and flat surfaces on the vessel in both the horizontal and vertical planes
 - Circles
 - Parabolas
 - Ellipsoids
 - Hyperbolas
 - Cones
- Implementation of robust regressions models suitable for this domain, based on RANSAC.

Metrics on Primary Features

- Measurements of features in the horizontal plane
- Measurements of features in the vertical plane
- Measurements of angles
- Measurements of volume

Exploration of Potential Design Ratios

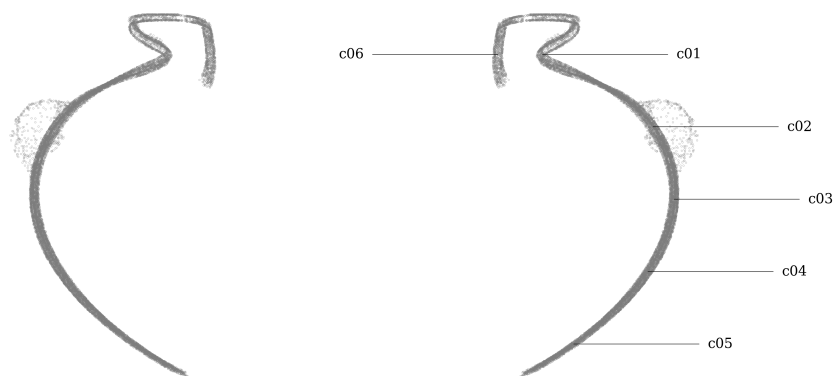
- π , φ , e , 1, 2, 3, 4 etc.

Raw Dataset Attachments

- Including all measurement and sample coordinates as CSV-files embedded in the report
- Including an STL file of the aligned object alongside the report, for easier external replication and validation of the research results

Appendix A - Comparison Of Circularity Measurements (Z-plane vs. surface-perpendicular)

Comparison of circularity samples



Samples perpendicular to the surface curvature

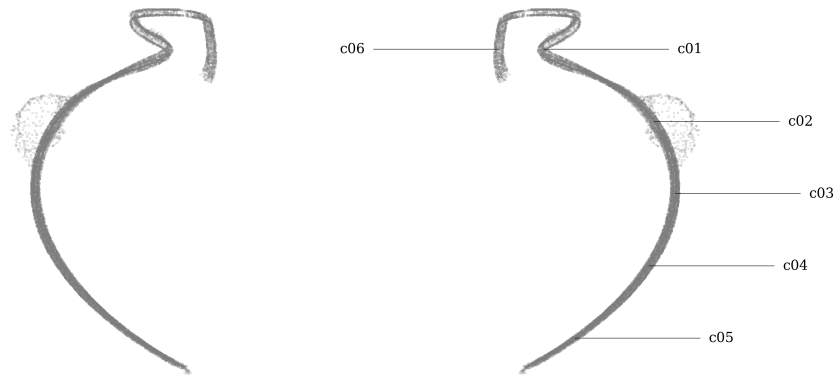
Tag	Area	Measured deviation ⁸	Residuals				Sample size	Slice		
			Range	RMSD ⁹	MAD ¹⁰	SD		Height	Z coord.	Radius ¹¹
		mm	mm	mm	mm	mm	mm	mm	mm	
c01	exterior	Ø42.190±0.667	1.113	0.329	0.268	0.329	1315	0.050	36.506	21.095
c02	exterior	Ø66.957±0.623	1.089	0.291	0.191	0.291	1286	0.050	28.418	33.478
c03	exterior	Ø71.663±0.506	1.000	0.282	0.241	0.282	2073	0.050	20.329	35.831
c04	exterior	Ø65.802±0.484	0.924	0.272	0.248	0.272	1656	0.050	12.241	32.901
c05	exterior	Ø49.198±0.432	0.706	0.148	0.099	0.148	850	0.050	4.152	24.599
c06	interior	Ø32.203±0.545	1.070	0.349	0.354	0.349	942	0.050	36.506	16.102

Table 7: Detailed circularity measurements at selected samples in z-plane, vessel MV018.

Samples in the Z-plane

Tag	Area	Measured deviation ⁸	Residuals				Sample size	Slice		
			Range	RMSD ⁹	MAD ¹⁰	SD		Height	Z coord.	Radius ¹¹
		mm	mm	mm	mm	mm	mm	mm	mm	
c01	exterior	Ø42.426±0.807	1.108	0.356	0.191	0.331	1257	0.050	36.506	21.213
c02	exterior	Ø67.061±0.842	1.364	0.362	0.245	0.359	2010	0.050	28.418	33.530
c03	exterior	Ø71.777±0.565	1.002	0.292	0.248	0.286	2114	0.050	20.329	35.889
c04	exterior	Ø65.695±0.601	1.156	0.326	0.283	0.322	2266	0.050	12.241	32.848
c05	exterior	Ø49.087±0.693	1.122	0.268	0.169	0.262	2526	0.050	4.152	24.543
c06	interior	Ø32.170±0.557	1.066	0.350	0.346	0.350	934	0.050	36.506	16.085

Table 8: Detailed circularity measurements at selected samples perpendicular to vessel curvature, vessel MV018.



Samples perpendicular to the surface curvature

Tag	Area	Measured deviation ⁸	Residuals				Sample size	Slice		
			Range	RMSD ⁹	MAD ¹⁰	SD		Height	Z coord.	Radius ¹¹
		in	in	in	in	in	in	in	in	
c01	exterior	Ø1.6610±0.0262	0.0438	0.0129	0.0106	0.0129	1315	0.0020	1.4373	0.8305
c02	exterior	Ø2.6361±0.0245	0.0429	0.0114	0.0075	0.0114	1286	0.0020	1.1188	1.3180
c03	exterior	Ø2.8214±0.0199	0.0394	0.0111	0.0095	0.0111	2073	0.0020	0.8004	1.4107
c04	exterior	Ø2.5906±0.0191	0.0364	0.0107	0.0098	0.0107	1656	0.0020	0.4819	1.2953
c05	exterior	Ø1.9369±0.0170	0.0278	0.0058	0.0039	0.0058	850	0.0020	0.1635	0.9685
c06	interior	Ø1.2678±0.0215	0.0421	0.0137	0.0139	0.0137	942	0.0020	1.4373	0.6339

Table 9: Detailed circularity measurements at selected samples in z-plane, vessel MV018.

Samples in the Z-plane

Tag	Area	Measured deviation ⁸	Residuals				Sample size	Slice		
			Range	RMSD ⁹	MAD ¹⁰	SD		Height	Z coord.	Radius ¹¹
		in	in	in	in	in	in	in	in	
c01	exterior	Ø1.6703±0.0318	0.0436	0.0140	0.0075	0.0130	1257	0.0020	1.4373	0.8352
c02	exterior	Ø2.6402±0.0332	0.0537	0.0143	0.0096	0.0141	2010	0.0020	1.1188	1.3201
c03	exterior	Ø2.8259±0.0222	0.0394	0.0115	0.0098	0.0113	2114	0.0020	0.8004	1.4129
c04	exterior	Ø2.5864±0.0237	0.0455	0.0128	0.0111	0.0127	2266	0.0020	0.4819	1.2932
c05	exterior	Ø1.9325±0.0273	0.0442	0.0105	0.0067	0.0103	2526	0.0020	0.1635	0.9663
c06	interior	Ø1.2665±0.0219	0.0420	0.0138	0.0136	0.0138	934	0.0020	1.4373	0.6333

Table 10: Detailed circularity measurements at selected samples perpendicular to vessel curvature, vessel MV018.

Comparison of circularity on the full vessel surface

Metric

Samples perpendicular to the surface curvature

Area	Range			Standard Deviation			Median Absolute Deviation			Slices	Slice height
	Median	Min.	Max.	Median	Min.	Max.	Median	Min.	Max.		
	mm	mm	mm	mm	mm	mm	mm	mm	mm		mm
Exterior	1.007	0.476	1.526	0.274	0.122	0.391	0.024	0.082	0.257	721	0.050
Interior	1.074	0.920	1.701	0.346	0.299	0.449	0.021	0.206	0.387	120	0.050

Table 11: Detailed circularity measurements at selected samples in z-plane, vessel MV018.

Samples in the z-plane

Area	Range			Standard Deviation			Median Absolute Deviation			Slices	Slice height
	Median	Min.	Max.	Median	Min.	Max.	Median	Min.	Max.		
	mm	mm	mm	mm	mm	mm	mm	mm	mm		mm
Exterior	1.142	0.985	3.055	0.310	0.260	0.837	0.024	0.164	0.723	719	0.050
Interior	1.074	0.938	1.669	0.345	0.309	0.450	0.019	0.211	0.399	119	0.050

Table 12: Detailed circularity measurements at selected samples perpendicular to vessel curvature, vessel MV018.

Imperial

Samples perpendicular to the surface curvature

Area	Range			Standard Deviation			Median Absolute Deviation			Slices	Slice height
	Median	Min.	Max.	Median	Min.	Max.	Median	Min.	Max.		
	in	in	in	in	in	in	in	in	in		in
Exterior	1.007	0.476	1.526	0.274	0.122	0.391	0.024	0.082	0.257	721	0.050
Interior	1.074	0.920	1.701	0.346	0.299	0.449	0.021	0.206	0.387	120	0.050

Table 13: Detailed circularity measurements at selected samples in z-plane, vessel MV018.

Samples in the z-plane

Area	Range			Standard Deviation			Median Absolute Deviation			Slices	Slice height
	Median	Min.	Max.	Median	Min.	Max.	Median	Min.	Max.		
	in	in	in	in	in	in	in	in	in		in
Exterior	1.142	0.985	3.055	0.310	0.260	0.837	0.024	0.164	0.723	719	0.050
Interior	1.074	0.938	1.669	0.345	0.309	0.450	0.019	0.211	0.399	119	0.050

Table 14: Detailed circularity measurements at selected samples perpendicular to vessel curvature, vessel MV018.

Circularity analysis of exterior samples perpendicular to surface curvature

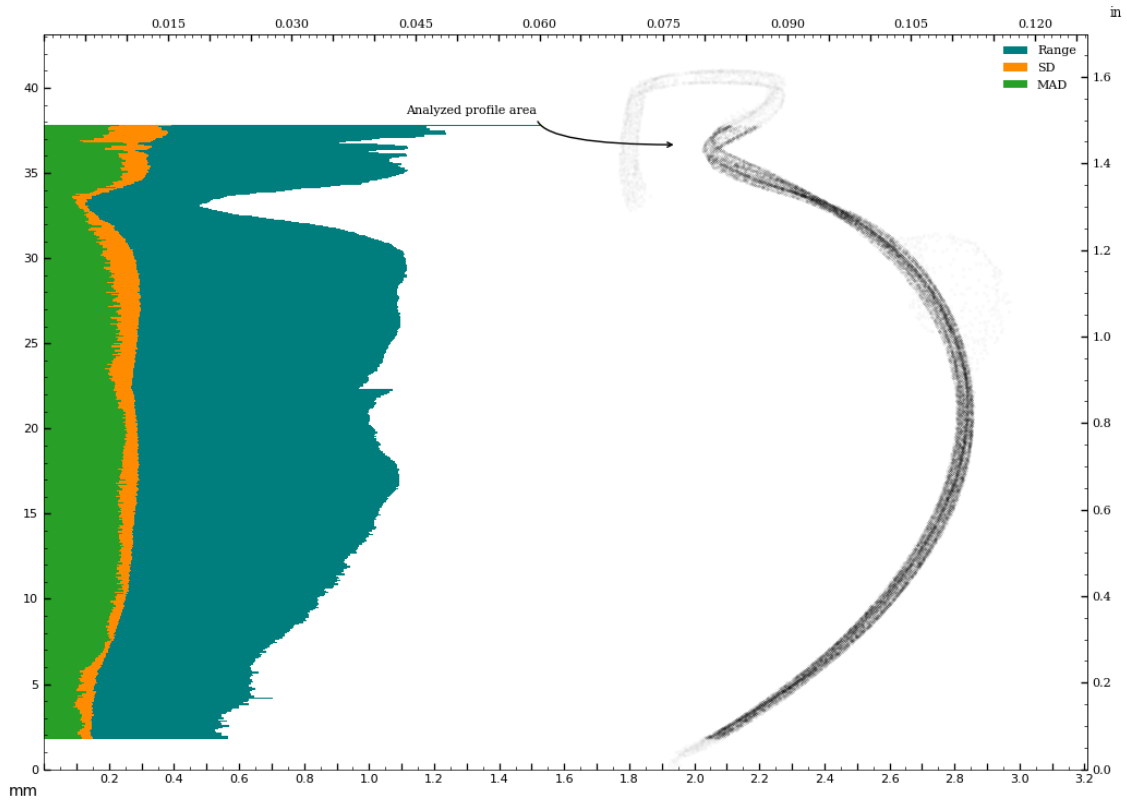


Figure 41: Circularity analysis of exterior samples perpendicular to surface curvature

Circularity analysis of exterior surface - in z-plane

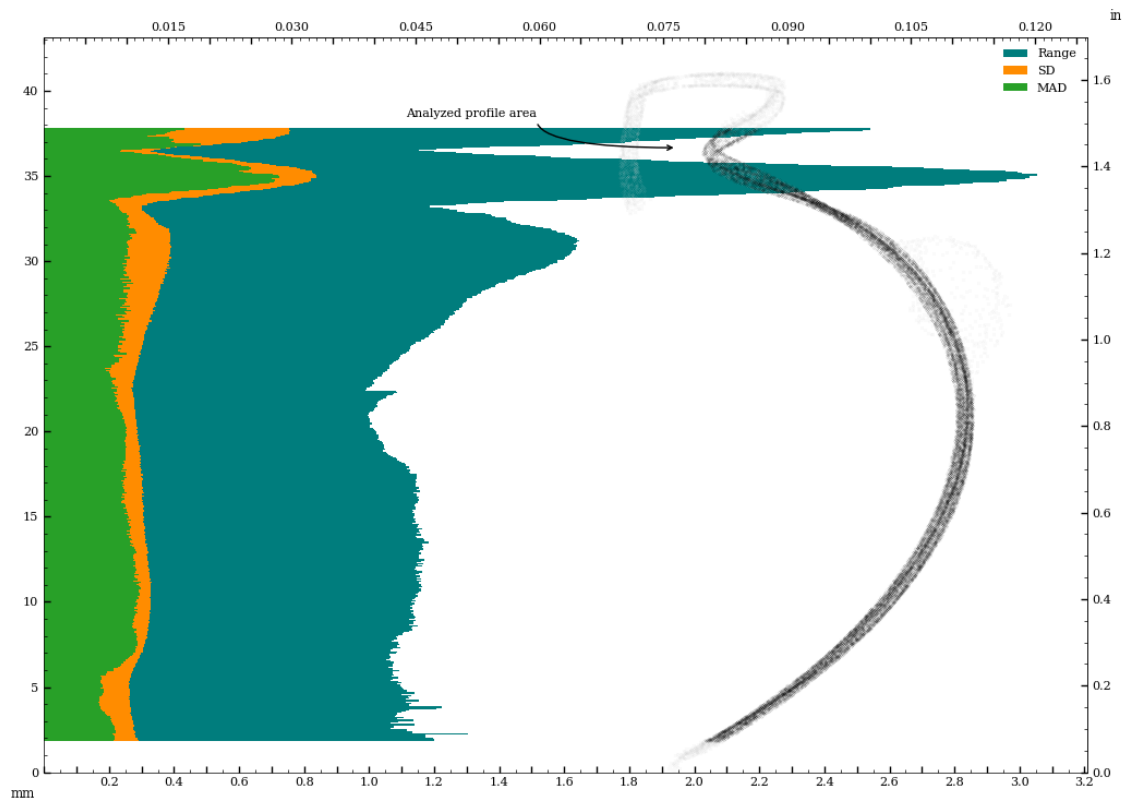


Figure 42: Circularity analysis of exterior surface - in z-plane

Circularity analysis of exterior samples perpendicular to surface curvature

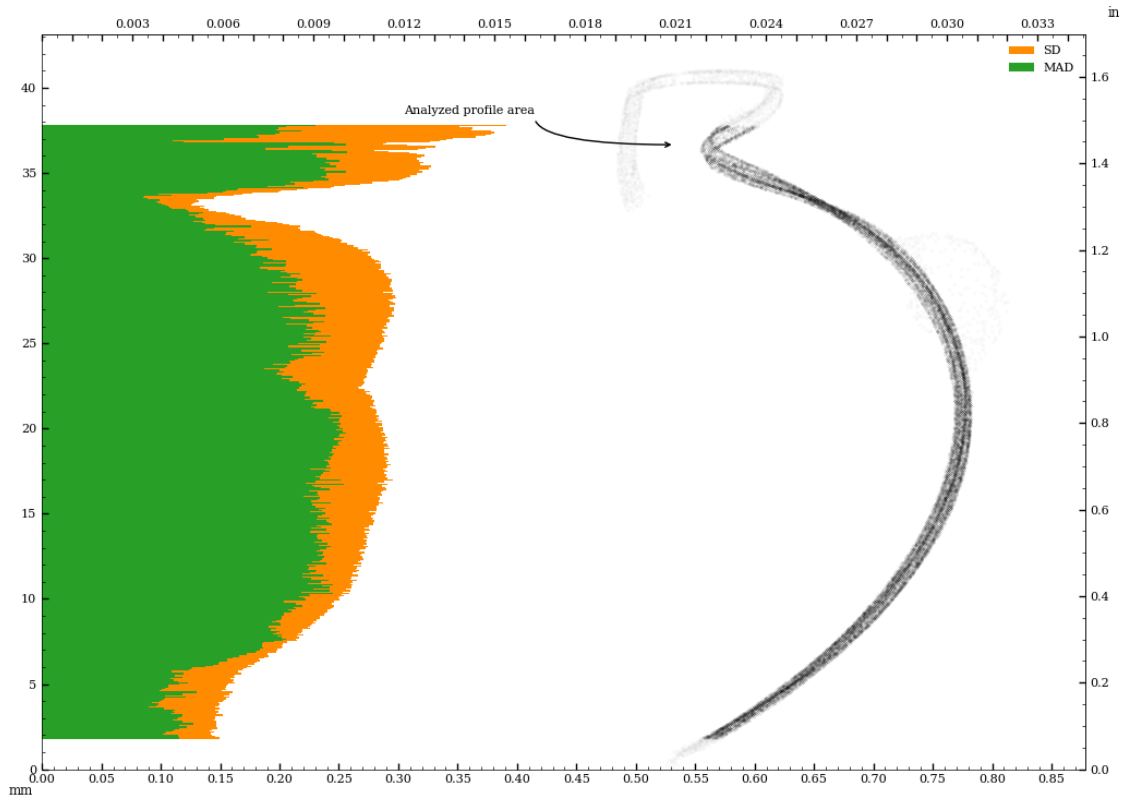


Figure 43: Circularity analysis of exterior samples perpendicular to surface curvature

Circularity analysis of exterior surface - in z-plane

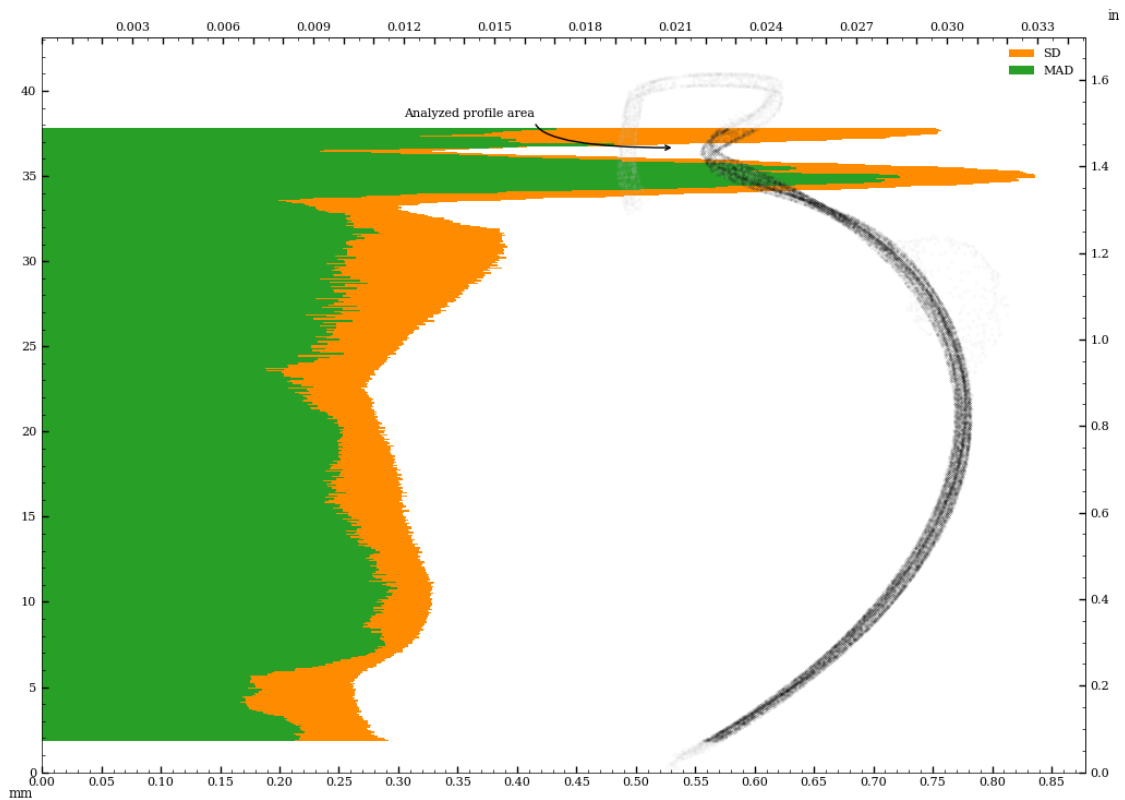


Figure 44: Circularity analysis of exterior surface - in z-plane

Circularity analysis of interior samples perpendicular to surface curvature

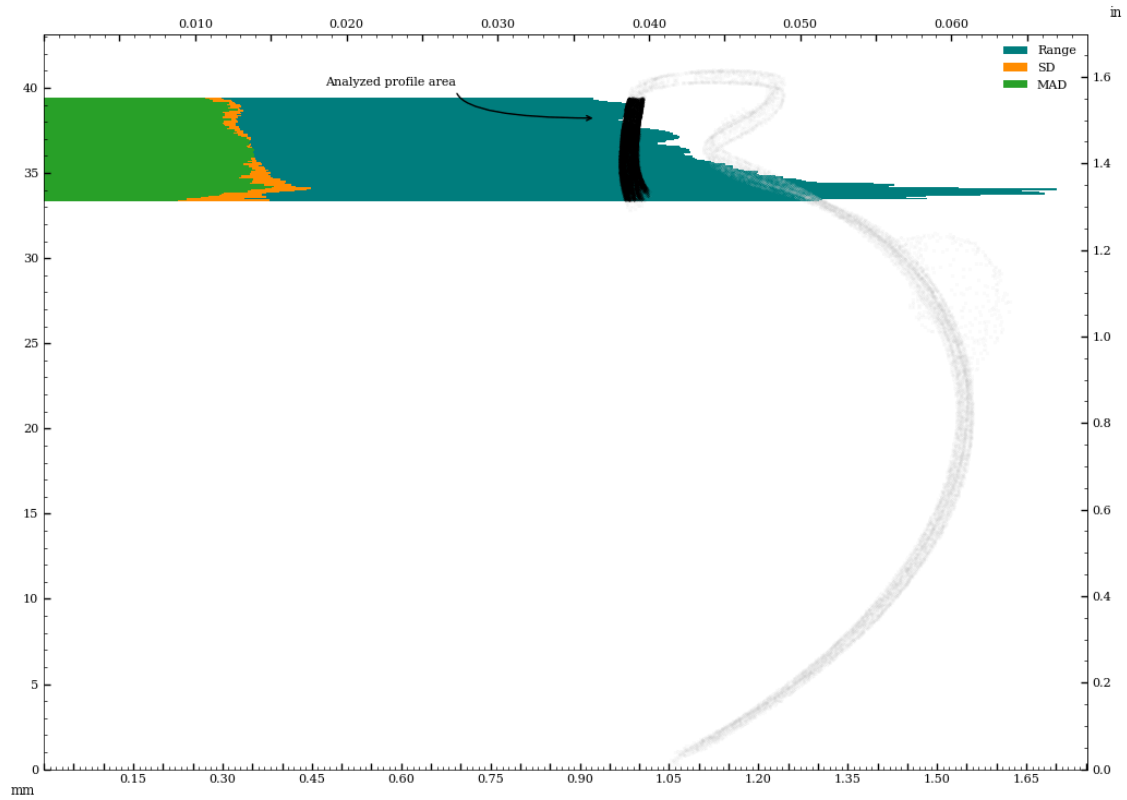


Figure 45: Circularity analysis of interior samples perpendicular to surface curvature

Circularity analysis of interior surface - in z-plane

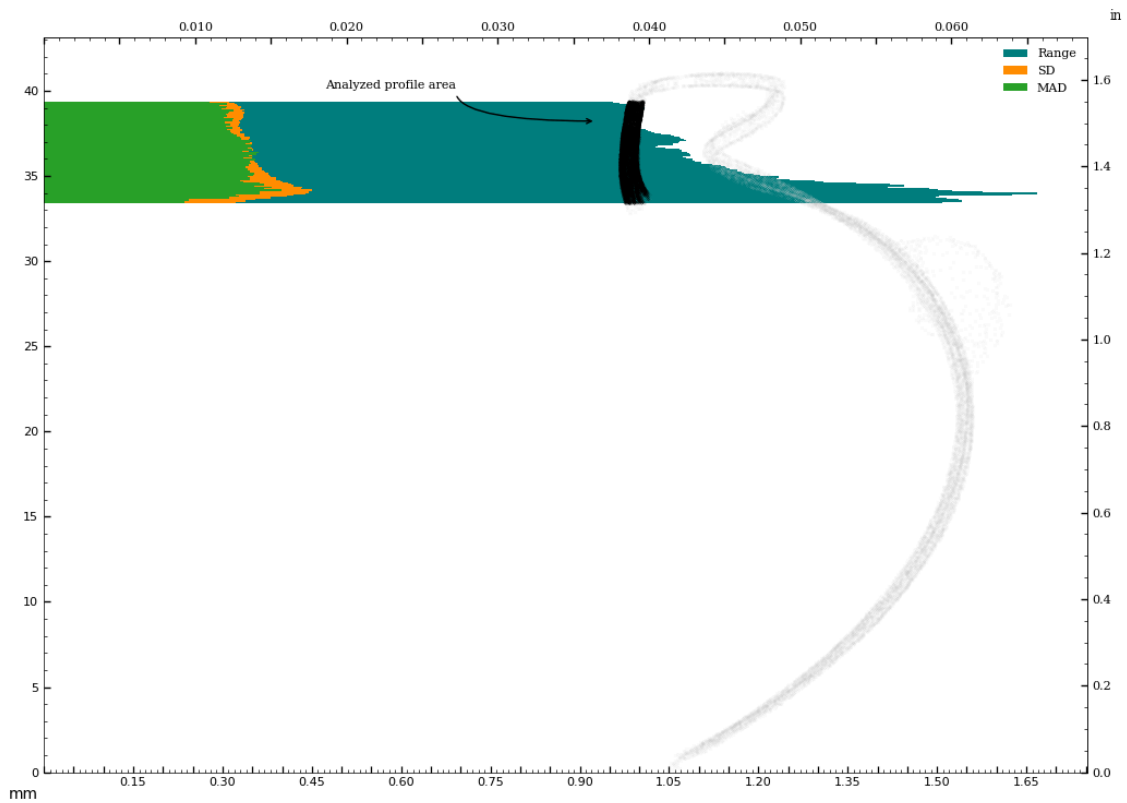


Figure 46: Circularity analysis of interior surface - in z-plane

Circularity analysis of interior samples perpendicular to surface curvature

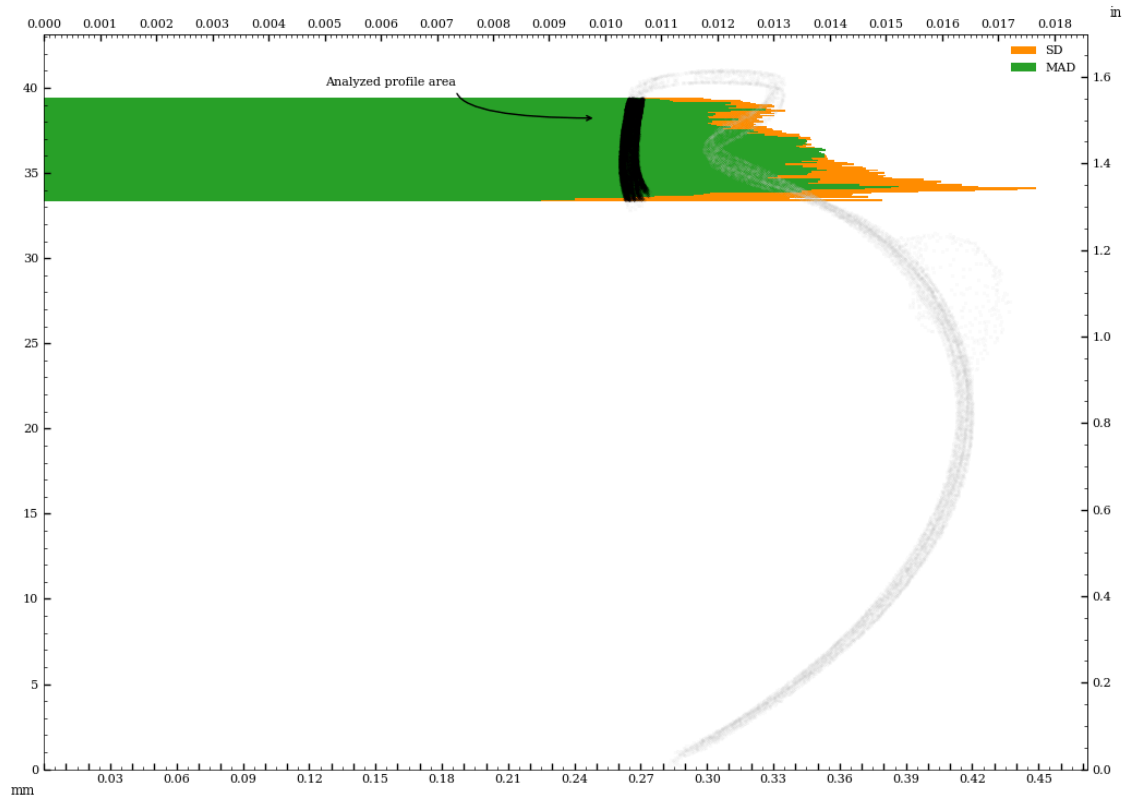


Figure 47: Circularity analysis of interior samples perpendicular to surface curvature

Circularity analysis of interior surface - in z-plane

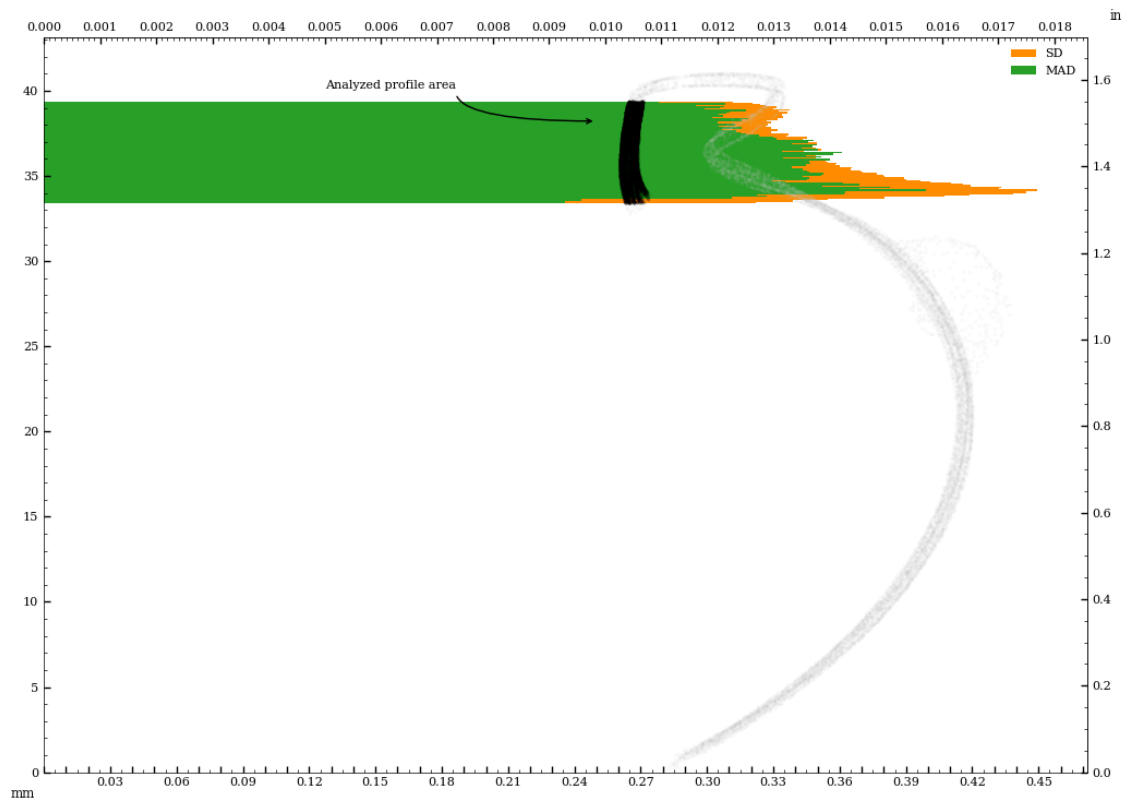


Figure 48: Circularity analysis of interior surface - in z-plane

Appendix B - Comparison Of Concentricity Measurements (Z-plane vs. surface-perpendicular)

Metric

Concentricity measurements perpendicular to surface curvature

Tag	Reference	Deviation	Sample size	Circle fit residuals analysis for sample listed in Tag column						
				Range full	Range inliers	SD full	SD inliers	MAD full	MAD inliers	Center (x,y)
		mm		mm	mm	mm	mm	mm	mm	μm
c01	z-axis	0.166	1487	1.074	1.074	0.335	0.335	0.251	0.251	-166, -17
c02	z-axis	0.117	1305	1.089	1.089	0.293	0.293	0.209	0.209	-4, -117
c03	z-axis	0.017	2078	1.000	1.000	0.282	0.282	0.247	0.247	-7, 16
c04	z-axis	0.012	1641	0.924	0.924	0.272	0.272	0.240	0.240	11, -5
c05	z-axis	0.087	850	0.706	0.629	0.147	0.146	0.096	0.096	-71, 51
c06	z-axis	0.487	942	1.070	1.070	0.349	0.350	0.348	0.355	-419, 248
c01	c06	0.366	1487	1.074	1.074	0.335	0.335	0.251	0.251	254, -265

Concentricity measurements in z-plane

Tag	Reference	Deviation	Sample size	Circle fit residuals analysis for sample listed in Tag column						
				Range full	Range inliers	SD full	SD inliers	MAD full	MAD inliers	Center (x,y)
		mm		mm	mm	mm	mm	mm	mm	μm
c01	z-axis	0.171	1460	1.166	1.166	0.343	0.343	0.287	0.287	-169, -29
c02	z-axis	0.173	2010	1.705	1.705	0.440	0.440	0.231	0.231	-15, -173
c03	z-axis	0.022	2114	1.047	1.047	0.287	0.287	0.252	0.252	-5, 22
c04	z-axis	0.019	2266	1.144	1.144	0.322	0.322	0.284	0.284	17, -6
c05	z-axis	0.268	2526	1.197	1.197	0.298	0.298	0.173	0.173	-206, 171
c06	z-axis	0.486	934	1.406	1.406	0.375	0.376	0.310	0.312	-418, 248
c01	c06	0.372	1460	1.166	1.166	0.343	0.343	0.287	0.287	249, -276

Imperial

Concentricity measurements perpendicular to surface curvature

Tag	Reference	Deviation	Sample size	Circle fit residuals analysis for sample listed in Tag column						
				Range full	Range inliers	SD full	SD inliers	MAD full	MAD inliers	Center (x,y)
		in		in	in	in	in	in	in	thou
c01	z-axis	0.0066	1487	0.0423	0.0423	0.0132	0.0132	0.0099	0.0099	-6.5, -0.7
c02	z-axis	0.0046	1305	0.0429	0.0429	0.0115	0.0115	0.0082	0.0082	-0.1, -4.6
c03	z-axis	0.0007	2078	0.0394	0.0394	0.0111	0.0111	0.0097	0.0097	-0.3, 0.6
c04	z-axis	0.0005	1641	0.0364	0.0364	0.0107	0.0107	0.0095	0.0095	0.4, -0.2
c05	z-axis	0.0034	850	0.0278	0.0248	0.0058	0.0058	0.0038	0.0038	-2.8, 2.0
c06	z-axis	0.0192	942	0.0421	0.0421	0.0137	0.0138	0.0137	0.0140	-16.5, 9.8
c01	c06	0.0144	1487	0.0423	0.0423	0.0132	0.0132	0.0099	0.0099	10.0, -10.4

Concentricity measurements in z-plane

Tag	Reference	Deviation	Sample size	Circle fit residuals analysis for sample listed in Tag column						
				Range full	Range inliers	SD full	SD inliers	MAD full	MAD inliers	Center (x,y)
		in		in	in	in	in	in	in	thou
c01	z-axis	0.0067	1460	0.0459	0.0459	0.0135	0.0135	0.0113	0.0113	-6.6, -1.1
c02	z-axis	0.0068	2010	0.0671	0.0671	0.0173	0.0173	0.0091	0.0091	-0.6, -6.8
c03	z-axis	0.0009	2114	0.0412	0.0412	0.0113	0.0113	0.0099	0.0099	-0.2, 0.8
c04	z-axis	0.0007	2266	0.0450	0.0450	0.0127	0.0127	0.0112	0.0112	0.7, -0.3
c05	z-axis	0.0106	2526	0.0471	0.0471	0.0117	0.0117	0.0068	0.0068	-8.1, 6.7
c06	z-axis	0.0191	934	0.0554	0.0554	0.0148	0.0148	0.0122	0.0123	-16.5, 9.7
c01	c06	0.0147	1460	0.0459	0.0459	0.0135	0.0135	0.0113	0.0113	9.8, -10.9